Geospatial Variation in Carbon Accounting of Low-Carbon Hydrogen Production Pathways: Implications for the Inflation Reduction Act

Valeria Vallejo[1], Quoc Nguyen[1], and Arvind P. Ravikumar*[1,2]

[1]Department of Petroleum and Geosystems Engineering, The University of Texas at Austin, Austin, TX USA
[2]Energy Emissions Modeling and Data Lab, The University of Texas at Austin, Austin, TX, USA

*Corresponding author email: arvind.ravikumar@austin.utexas.edu

Abstract

Low-carbon hydrogen is considered a key component of global energy system decarbonization strategy. The US Inflation Reduction Act includes incentives in the form of production tax credits for low-carbon hydrogen production, provided the lifecycle greenhouse gas (GHG) emissions intensity (EI) of hydrogen is below 4 kg CO2e/kg H2. Blue hydrogen or hydrogen produced from natural gas coupled with carbon capture and sequestration is one such pathway. In this work, we develop a geospatial, measurement-informed model to estimate supply chain specific lifecycle GHG EI of blue hydrogen produced with natural gas sourced from the Marcellus and Permian shale basins. We find that blue hydrogen production using Permian gas has a lifecycle EI of 7.4 kg CO2e/kg H2, more than twice the EI of hydrogen produced using Marcellus gas of 3.3 kg CO2e/kg H2. We conclude that eligibility for tax credits should therefore be based on lifecycle assessments that are supply chain specific and measurement informed to ensure blue hydrogen projects are truly low carbon.

Hydrogen is at the peak of technology hype cycles[1]. Recent pronouncements have declared hydrogen to be the solution to the decarbonization challenge in heavy industry, agriculture, power sector, shipping, and aviation[2–7]. Governments around the world, led by the European Union and now the United States, have invested billions of dollars in jumpstarting a hydrogen economy[8–10]. Even as potential applications of clean hydrogen continue to expand, demand for hydrogen in traditional applications such as fertilizer manufacturing and industry is expected to increase[11]. In parallel, energy system models of a net-zero economy by 2050 continue to suggest hydrogen as a key component of the global economy[12–15]. Much of the hydrogen produced in the world are from fossil fuels such as coal or natural gas through steam methane reforming, with a greenhouse gas (GHG) emissions intensity of 20 – 25 kg CO2e/kg H2 or 10 – 15 kg CO2e/kg H2, respectively[16–18]. A large role for hydrogen in a decarbonized world requires urgent development and scale up of low and zero-carbon hydrogen production systems. In practice, the most likely candidate technologies include gas-based hydrogen production with carbon capture and sequestration (CCS), also called blue hydrogen, or electrolysis using clean electricity, also called green hydrogen[18,19].

The US Department of Energy recently announced the creation of seven hydrogen hubs across the country, each receiving approximately $1 billion to accelerate the commercial-scale deployment of clean hydrogen[8]. At least three of the announced hubs plan to produce low-carbon hydrogen from natural gas using CCS. In addition to federal investments in kickstarting a national clean hydrogen ecosystem, the Inflation Reduction Act (IRA) provided tax credits for clean hydrogen production[20]. The production tax credit (hereafter referred to as the 45V PTC) is available on a graded scale of the lifecycle GHG emissions intensity, with a minimum credit of $0.60 per kg of H2 up to a maximum of $3 per kg of H2. For comparison, recent estimates of costs of hydrogen production using clean energy-based electrolysis and fossil fuel-based steam methane reforming were in the range of $6-10 /kg H2 and $1-4 /kg H2, respectively[17,18]. Whether a project is eligible for the full 45V PTC depends on the well-to-gate lifecycle GHG emissions intensity as estimated by Argonne National Lab's greenhouse gases, regulated emissions, and energy use in technologies (GREET) model[21].

Several recent studies have estimated the lifecycle GHG emission intensity of hydrogen production pathways[16–18,22,23]. Estimates of blue hydrogen emissions intensity range from 3 – 9 kg CO2e/kg H2, with the variability attributed to assumptions around supply chain methane emissions and capture efficiency. A common theme across all studies is the use of nationally representative estimates for key model parameters such as average electricity grid carbon intensity or national average methane emission rate. For example, the GREET model uses a base case assumption of a nationally representative 1% methane leakage across US natural gas supply chains to estimate GHG intensity of blue hydrogen production. Recent work on the design of the 45V PTC for low-carbon electrolytic hydrogen production showed that verification and assurance of low carbon attributes require stringent conditions to be imposed on time matching and additionality of clean electricity[24].

The use of nationally representative parameter estimates for supply chain methane emissions and other variables in a lifecycle framework is insufficient to estimate the GHG emissions intensity of blue hydrogen production in the US. Measurements of methane emissions over the past decade have identified significant spatio-temporal variability in emissions at different scales[25–31]. Field campaigns in the Permian basin in Texas and New Mexico alone have reported methane emissions ranging from a production normalized estimate of 3.7% to 9.4%[32–34]. By contrast, recent aerial-

based measurements in the Marcellus shale basin in Pennsylvania showed a methane emission rate of less than 1%[35–37]. In addition to spatial variation in emissions, analysis of recent measurements demonstrates that official methane emissions inventories such as the US Environmental Protection Agency (EPA) GHG Inventory underestimate methane emissions by 60%[25,38]. Yet, most LCA studies of natural gas and blue hydrogen typically use EPA GHG inventory estimates of emissions because of a lack of standardization in reporting across measurement studies[39–42]. To accurately estimate lifecycle emissions of blue hydrogen production in the US, it is critical to use measurement-informed emissions inventories[29,43,44].

Differences in supply chain methane emissions, although significant on their own, are just one of several key differences in emissions associated with the natural gas supply chain. For example, the degree of electrification affects the amount of grid-based electricity that is consumed across the supply chain at processing facilities and transmission compressor stations. The Marcellus shale basin, with a relatively high degree of electrification compared to the Permian basin, uses significantly more electricity to power major processes. However, because of the coal-heavy electricity grids in Ohio and West Virginia where much of the natural gas processing facilities are located, embodied emissions associated with the use of grid electricity is higher for the Marcellus basin compared to the Permian basin. Thus, modeling the GHG emissions intensity of hydrogen production using national average estimates is unlikely to be representative of any real-world hydrogen production facility in the US.

In this work, we develop a geospatial lifecycle assessment model to create supply-chain specific estimates of the well-to-gate GHG emissions intensity of blue hydrogen production. We assume hydrogen is produced using steam methane reforming (SMR) techniques and include emissions associated with capture, transport, and sequestration of CO2 from the hydrogen production facility within lifecycle system boundaries. Our work represents two key advances: one, it creates a spatially explicit framework that helps assess the environmental impacts of supply chain specific hydrogen production, and two, it incorporates measurement informed GHG emissions inventory within the lifecycle framework that addresses systemic emissions underestimation in official inventory estimates. We demonstrate the impact of these two advances using case studies of blue hydrogen production in Ohio and Texas using natural gas derived from the Marcellus and Permian basin, respectively. With the 45V PTC being available for any hydrogen project over the next decade, whether the US creates a truly low-carbon hydrogen ecosystem will critically depend on our ability to accurately estimate project-based and supply-chain specific lifecycle GHG emissions intensity.

Results

Figure 1 shows the LCA boundary and relevant material flows through various life cycle stages. The functional unit for this analysis is 1 kilogram of hydrogen production, thus the results are given in units of kg CO_2e/kg H_2. Emissions are aggregated using 100-year global warming potential (GWP) for methane from the Sixth Assessment Report of the IPCC (20-year GWP analysis is presented in Table S2). In this analysis, we do not consider the GHG emissions impact of hydrogen leakage because our supply chain boundary ends at the hydrogen production facility. This choice enables our results to serve as a benchmark for the 45V PTC since the foundation for the tax credit provisions is a well-to-gate LCA that excludes emissions from hydrogen

transportation and use. Recent work on modeling global warming potential (GWP) of hydrogen has typically resulted in values between 1 and 10[45,46]. Analysis of hydrogen in end use sectors such as transportation or power generation should include hydrogen leakage from point of production through end use.

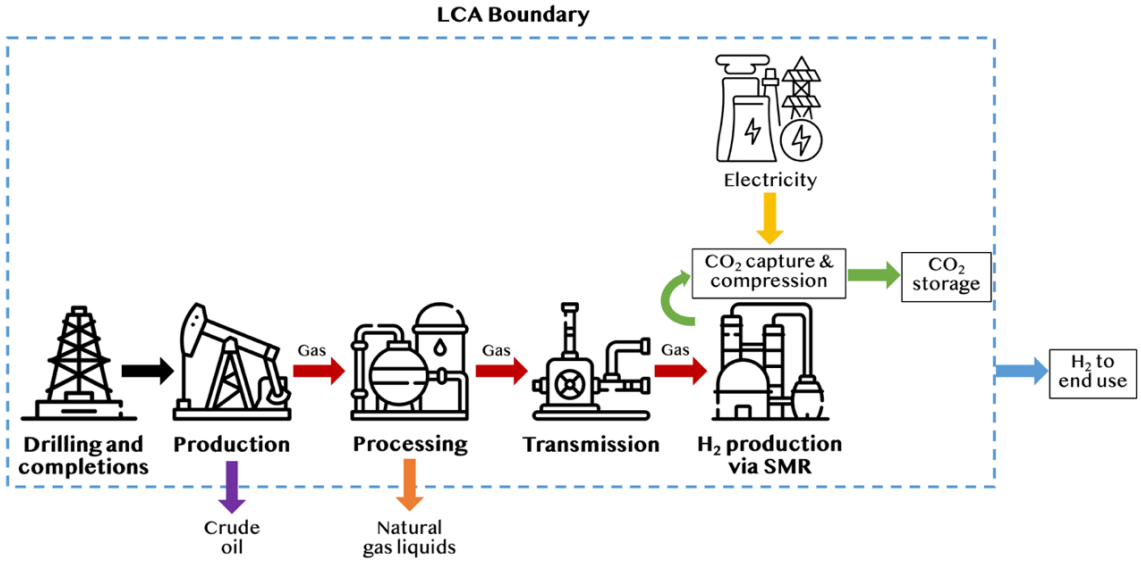

Figure 1. Life cycle assessment boundary for blue hydrogen production pathways in this study, including material flows of crude oil (purple), natural gas (red), and natural gas liquids (orange). Carbon capture and sequestration and electricity use are show in green and yellow, respectively.

Figure 2 shows the energy flows along the natural gas supply chain to produce 1 kg H2, accounting for all losses from methane emissions and flaring, and process fuel consumption. To produce 1 kg of H2, the input energy that must be extracted in the Permian basin is nearly 2.5 times that required in the Marcellus basin. 1 kg H2 produced using natural gas sourced from the Marcellus basin requires 317 MJ of energy extracted, corresponding to a supply chain energy conversion efficiency of 45%. By contrast, 1 kg of H2 produced using natural gas sourced from the Permian basin requires 788 MJ of energy extracted, corresponding to a supply chain energy conversion efficiency of 18%. The lower conversion efficiency in the Permian basin compared to the Marcellus basin can be attributed to two key factors: one, difference in resource composition resulting from co-production of crude oil and natural gas liquids across the two basins, and two, differences in supply chain methane emissions. In the southwest Marcellus basin, co-products include dry natural gas and natural gas liquids (NGLs). In the Permian basin, co-products include crude oil, dry natural gas, and NGLs. Because of the higher energy density of crude oil, much of the extracted energy from the Permian basin is embedded in crude oil, resulting in a lower energy conversion efficiency.

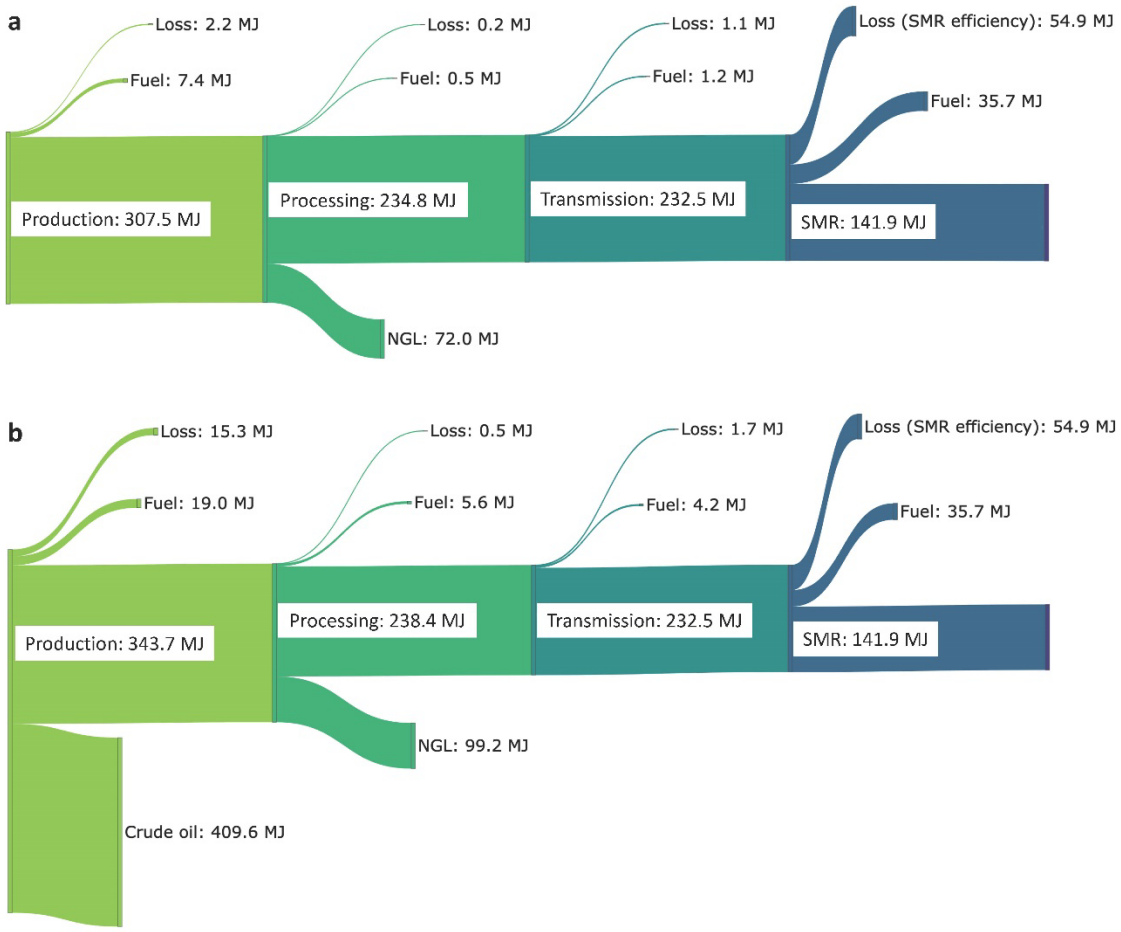

Figure 2. Energy flows of dry natural gas and co-products of crude oil and natural gas liquids across blue hydrogen production pathways using natural gas sourced from the (a) Marcellus basin, and (b) Permian basin. Losses correspond to methane emissions across the natural gas supply chain including leaks, venting, and flaring, and fuel consumption corresponding to gas use across various process stages.

Figure 3 shows the difference in the life cycle GHG emissions intensity of blue hydrogen production from the Marcellus and Permian shale basins. Two scenarios are modeled for each production region: a base case scenario that considers CO2 capture from both the SMR by-product and fuel combustion required to operate the SMR plant and an SMR-only scenario that considers CO2 capture only from the SMR by-product but not CO2 emissions associated with fuel combustion to operate the SMR plant. These two scenarios are explicitly modeled because the two capture processes require different solvents to absorb CO_2, thus requiring two different absorbent columns (methods).

Results from the base case indicate that H2 produced from Marcellus gas has a life cycle emissions intensity of 3.3 kg CO_2e/kg H_2. By contrast, H2 produced from Permian gas has a life cycle GHG emissions intensity of approximately 7.4 kg CO_2e/kg H_2, over twice that of hydrogen

produced from Marcellus gas. For jurisdictions such as New York state that require the use of 20-year GWP in environmental impact analysis, the life cycle emissions for the Marcellus and Permian-based blue H2 production increases to 6.4 and 16.9 kg CO_2e/kg H_2, respectively (see SI Tables S10 and S11 for 20-year and 100-year GWP-based emissions intensity).

Life cycle GHG emissions intensity are higher for the SMR-only carbon capture scenario. Figure 3b shows the increase in life cycle GHG emissions without post-combustion CO_2 capture. For the Marcellus gas based blue H2, the life cycle GHG emissions intensity increases by 45% to 4.8 kg CO_2e/kg H_2. Similarly, life cycle GHG emissions intensity for the Permian-based blue H2 production increases by 18% to 8.7 kg CO_2e/kg H_2. In both scenarios, we assume electricity emissions associated with average grid emissions factors in Texas and Ohio for the Permian and Marcellus-based supply chains, respectively. If hourly-matched zero carbon electricity is available to power the SMR and carbon capture plant, the life cycle GHG emissions intensity for the Marcellus and Permian-based H2 production decreases to 2.6 kg CO_2e/kg H_2 and 6.9 kg CO_2e/kg H_2, respectively, compared to the base-case scenario (see SI figure S3).

There are two key root causes for the difference in emissions intensity between the two H2 production supply chains: (1) higher upstream and midstream methane emissions in the Permian supply chain compared to the Marcellus supply chain, and (2) differences in product streams from the two basins. Recent top-down methane measurements in the Permian basin indicate a significantly higher average production-normalized emission rate compared to the Marcellus shale. Midstream emissions associated with transmission compressor stations are larger for the Permian basin because of the distance between the gas processing facilities in West Texas and demand centers in Southeast Texas, requiring more compressor stations to transport the gas (Methods). By contrast, the distance between the gas processing facility in Southwest Pennsylvania for the Marcellus basin is relatively closer to demand centers in Ohio, requiring fewer compressor stations for gas transport. Additionally, emissions from the natural gas supply chain are apportioned on an energy-based and product assigned allocation basis, which varies by basin because of differences in co-products. The Marcellus shale only produces dry gas and NGLs while the Permian basin produces crude oil, natural gas, and NGLs (methods).

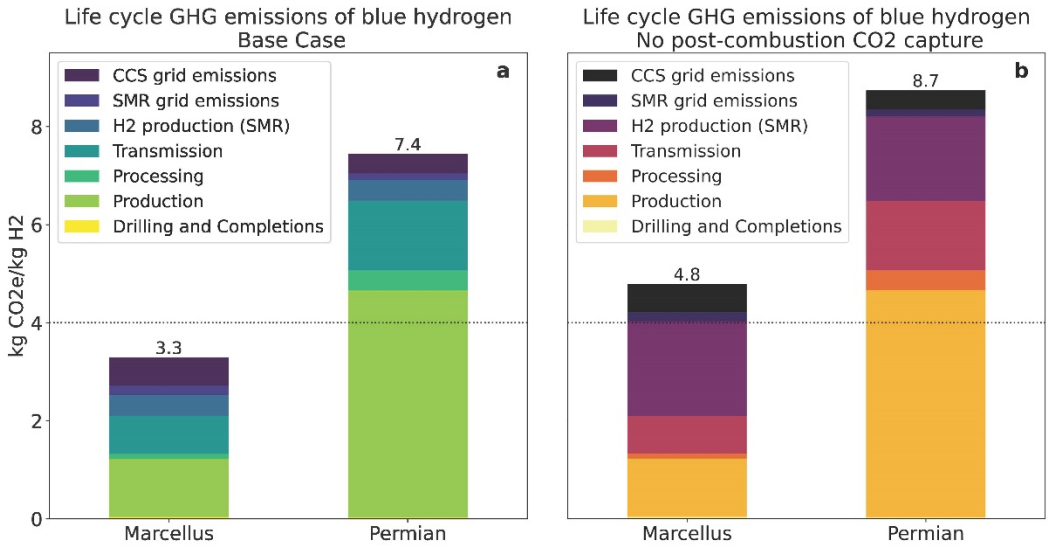

Figure 3. Lifecycle GHG emissions intensity in kg CO2e/kg H2 associated with blue hydrogen production using natural gas from the Marcellus shale and Permian shale basin for (a) base case scenario with post-combustion CO2 capture and (b) without post-combustion CO_2 capture. Emissions are disaggregated across life cycle stages (methane expressed in kg CO_2e based on GWP of 100-year horizon from IPCC AR6). The dotted line represents the threshold emissions intensity to qualify for the clean hydrogen production tax credits in the Inflation Reduction Act.

Impact of methane leakage and carbon capture rate on lifecycle blue H2 emissions intensity

Recent measurement campaigns across the US have demonstrated that methane emissions vary by facility, operator, region, and basin, often by an order of magnitude. Because of large uncertainties in measurement-based methane emission estimates and efficiency of carbon capture processes, it is instructive to quantify the impact of these two key variables on emissions intensity of blue H2. This sensitivity analysis addresses two key challenges. First, it provides a quantitative tool to evaluate the eligibility of blue hydrogen for 45V PTC to determine benchmarks for methane emissions rate and carbon capture efficiency[20]. Second, it identifies trade-offs between reducing methane leakage or improving capture efficiency in reducing emissions intensity of blue H2, relative to green hydrogen. This addresses principal agent issues – the entity developing the blue hydrogen project may only have direct control over capture technology (and therefore capture efficiency) and will be unable to significantly reduce supply chain methane emissions in the absence of a robust, domestic differentiated gas market[44].

Figure 4 shows the effect of both methane emission rate and carbon capture efficiency on the total lifecycle GHG emissions of blue hydrogen production. Four scenarios are analyzed: (a) Marcellus gas-based hydrogen using average emissions intensity of electricity in Ohio, (b) Permian gas-based hydrogen using average emissions intensity of electricity in Texas, (c) Marcellus gas-based hydrogen using hourly matched, zero-carbon electricity from wind, and (d) Permian gas-based hydrogen using hourly matched, zero-carbon electricity from wind. The use of clean

electricity to run the blue hydrogen plants in Ohio and Texas increases the allowable design space of supply chain methane leakage and capture rate by reducing overall emissions intensity of blue H2. Thus, eligibility for the 45V PTC in the IRA for blue hydrogen depends on three key variables: supply chain methane leakage, carbon capture rate, and carbon intensity of electricity.

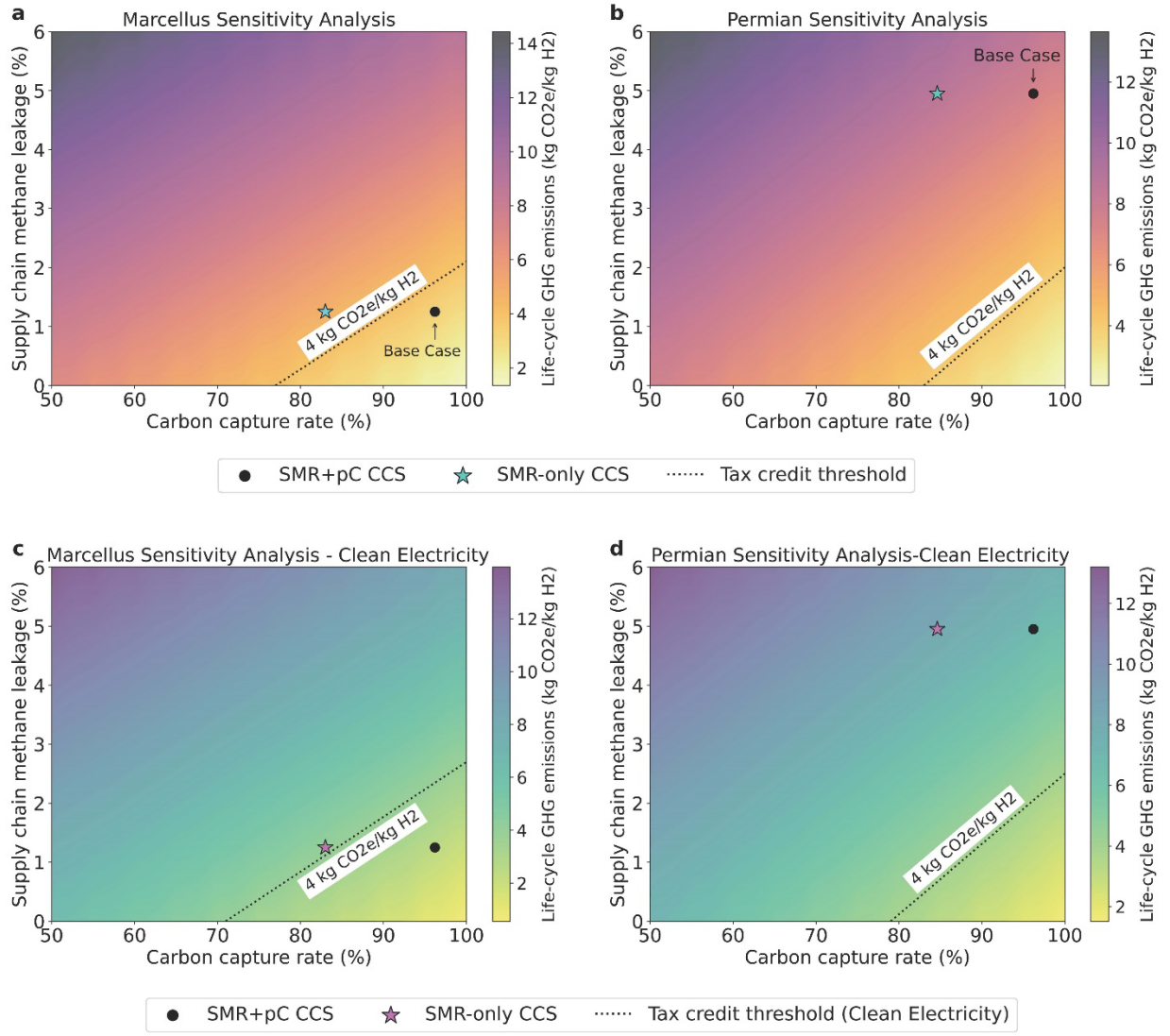

Figure 4. Impact of carbon capture rate (%) and supply chain methane emissions rate (%) on the life cycle GHG emissions intensity of blue hydrogen production from the Marcellus (left) and Permian basin (right). The dotted line represents the threshold of 4 kg CO2e/kg H2 to qualify for 45V PTC in the IRA. The black dot represents the life cycle emissions of the base case scenario (pre- and post-combustion capture and use of grid electricity), and the stars represent the scenario without post-combustion carbon capture. Panels (a) and (b) assume electricity emissions based on average grid emissions factors, while panels (c) and (d) assume the availability of hourly matched, zero emissions clean electricity.

Results from the base case indicate that only blue hydrogen produced from gas derived from the Marcellus shale with an emissions intensity of 3.3 kg CO2e/kg H2 will qualify for the 45V PTC, up to 20% of the maximum PTC of $3 per kg H2. Furthermore, blue hydrogen produced from the Marcellus shale does not qualify for any tax credits if the emissions from fuel combustion for the SMR are not captured. This increase in GHG emissions emphasizes the need for capturing not only the CO_2 by-product from SMR but also the CO_2 resulting from fuel combustion; otherwise, hydrogen from the Marcellus case is unlikely to quality under this tax credit provision. The use of hourly-matched clean electricity further reduces the emissions intensity of Marcellus gas based blue H2 to 2.6 kg CO2e/kg H2, making it eligible for at least 20% of the maximum PTC. Efforts to reduce supply chain methane leakage to about 0.5% – as some recent studies have shown – could further reduce emissions intensity to between 0.45 and 2.6 kg CO2e/kg H2. This would allow Marcellus gas based blue H2 projects to be eligible for up to 33% of the maximum PTC.

By contrast, Permian gas based H2 does not qualify for the H2 PTC in the IRA in any of the three scenarios: base case, no post-combustion CO_2 capture, and clean electricity use. The only scenario where hydrogen produced from natural gas sourced from the Permian basin could qualify for tax credit provisions is if the total production-normalized supply chain methane emissions rate is reduced to 2% or less, depending on overall CO2 capture rate. Furthermore, there is no scenario that only increases capture efficiency without addressing supply chain methane emissions that would make Permian gas based blue H2 eligible for 45V PTC. Thus, entities that want to develop blue H2 facilities in the Gulf Coast using gas sourced from the Permian basin will need comprehensive strategies to address supply chain methane emissions.

In both the Marcellus and Permian gas based blue hydrogen, it is unlikely that any project will be eligible for the maximum PTC in the IRA of $3/kg H2, which requires an emissions intensity below 0.45 kg CO2e/kg H2. Achieving this in the context of blue H2 production requires advanced monitoring, widespread electrification, and large-scale equipment replacement programs in developing near-zero methane leakage across natural gas supply chains.

Comparison of life cycle GHG emissions from blue hydrogen production with other hydrogen production pathways

Figure 5 shows a comparison of life cycle GHG emissions intensity of blue hydrogen from this study with other hydrogen production pathways in the literature[47–54]. Green or zero-carbon hydrogen has some of the lowest GHG emissions intensity due to the use of electrolysis powered by renewable energy to produce hydrogen. However, these low emissions are a function of the electricity generation mix and hourly matching constraints powering the electrolysis. For example, if the electrolyzers are connected to the local electric grid, GHG emissions will depend entirely on the average emissions intensity of the location-specific grid mix. Kleijne et al. argued that electrolyzers obtain power from the average power mix of the grid that it is connected to unless additional renewable energy capacity is guaranteed[48]. Recent analyses have argued for stringent US Treasury guidelines for clean hydrogen including hourly matching of electrolyzer energy needs with additional clean energy deployed for hydrogen production[24]. We estimate the emissions of grid-connected, electrolyzer-based hydrogen production in both Ohio and Texas to compare it to our case studies. Emissions from grid-connected hydrogen production are 30.3 kg CO_2e/kg H_2 in

Ohio and 21.5 kg CO_2e/kg H_2 in Texas, which are significantly higher than blue hydrogen produced in these states. These high emissions intensities for grid-connected hydrogen production arise from the high energy needs of the electrolysis process, estimated to be about 55 kWh/kg H2.

Emissions of green hydrogen produced from 100% renewables can also depend on the type of renewable source; for instance, hydrogen produced with wind power and photovoltaic (PV) cells have life cycle GHG emissions of 0.55 and 4.4 kg CO_2e/kg H_2, respectively. These life cycle emissions include the emissions associated with the manufacturing of wind turbines or solar cells. The only hydrogen production technology that is comparable to green hydrogen produced with wind power in terms of low life cycle GHG emissions is hydrogen produced with nuclear energy[47].

Currently, fossil fuels dominate hydrogen production since they constitute approximately 96% of the global feedstock used for hydrogen production. However, emissions associated with brown and grey hydrogen are substantially higher than those from clean energy and nuclear-based hydrogen. Hydrogen produced from fossil fuels without carbon capture have emissions intensity between 10 – 30 kg CO2e/kg H2 due to the release of CO2 from SMR into the atmosphere. Similarly, coal-based hydrogen has one of the highest emissions intensities in the literature of 25 kg CO2e/kg H2, similar to the highest gas-based hydrogen production[52]. For gas-based hydrogen production to be eligible for carbon credits, it requires either effective methane emission mitigation and high capture efficiency (blue hydrogen) or the use of methane pyrolysis[53]. Indeed, recent studies have shown that low-carbon blue hydrogen and green hydrogen production can be cost-competitive with carbon-intensive gray hydrogen[55]. Our work demonstrates that the low emissions feature of blue hydrogen is highly location specific and must be carefully assessed on a project-by-project basis.

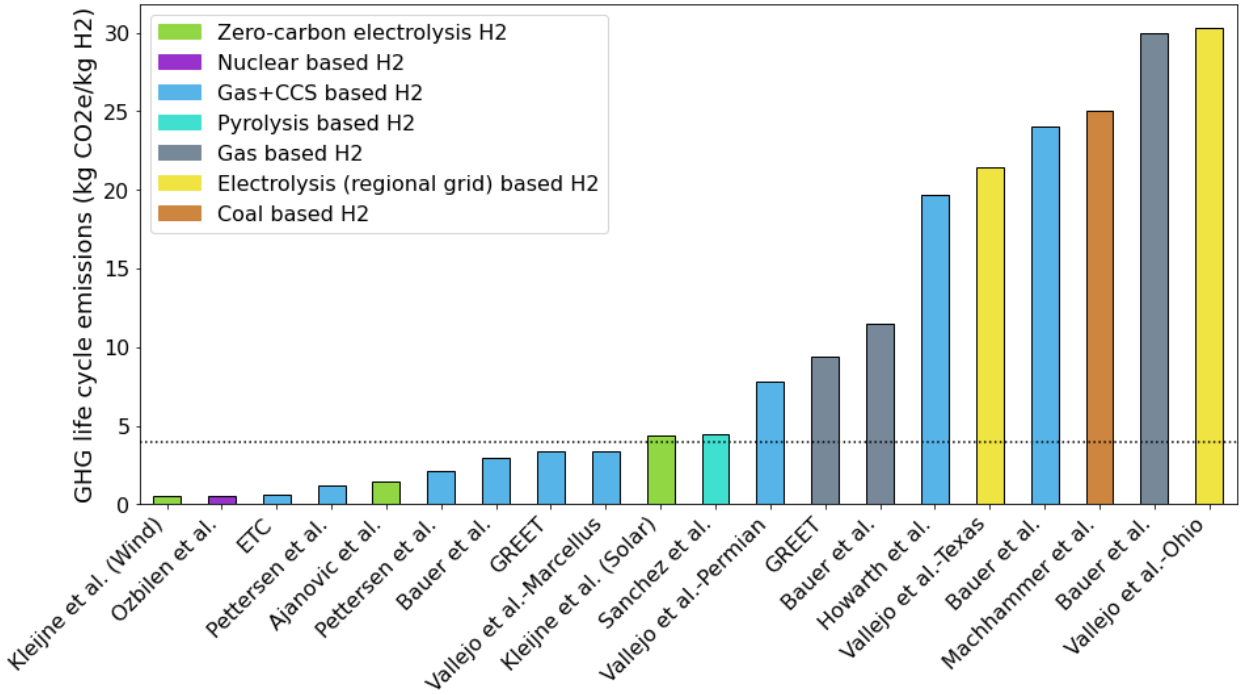

Figure 5. Comparison of life cycle GHG emissions intensity of various hydrogen production technologies from existing literature in comparison with results from this study. The dotted line

represents the 4 kg CO2e/kg H2 threshold to qualify for clean hydrogen production tax credits in the Inflation Reduction Act.

Discussion and Conclusions

In this work, we developed a geospatial LCA of blue hydrogen production pathways using natural gas sourced from the Marcellus and Permian basin. We demonstrate the impact of spatial differences in GHG emissions across US natural gas supply chains on lifecycle emissions intensity of blue hydrogen production. Thus, eligibility for the hydrogen 45V PTC in the IRA – which is based on a lifecycle emissions intensity calculation – should be project-specific and location dependent to ensure tax credits go to truly low-carbon projects. We draw three primary conclusions from our analysis.

Location matters. Recent evidence from direct measurements across the oil and gas supply chain demonstrates the large spatio-temporal variation in methane emissions. These emissions directly affect the life cycle GHG emissions intensity of blue hydrogen – results from our study indicate at least a 2x difference between the Permian and Marcellus basins. Crucially, using a nationally averaged methane emission rate to determine average GHG emissions intensity of blue H2 production is unlikely to be representative of *any* blue H2 production facility. Guidelines to determine eligibility for H2 PTC should be based on regional or basin-specific modeling of the supply chain for natural gas. Significant expansion in methane measurement campaigns across the US over the past decade has made data on basin-specific emissions estimates readily available. Updating conventional LCA models such as GREET or National Energy Technology Laboratory's liquefied natural gas LCA model using basin-specific, measurement-informed emissions inventory can enable analyses of blue H2 production pathways that are representative of US operations.

Levers available to blue hydrogen project developers to reduce emissions vary by location. In theory, there are three levers to reduce emissions intensity of H2 production – supply chain methane emissions, capture efficiency, and electricity source for hydrogen production. However, the importance of these levers varies by location. In the Marcellus basin with relatively low methane emissions, all three levers can meaningfully reduce emissions with the most impact attributable to the use of clean electricity instead of grid electricity to power the SMR facility (coal is a significant part of the grid mix in Ohio). However, in the Permian basin, no amount of clean electricity or improved capture efficiency can mitigate the effects of high supply chain methane emissions. Thus, without significant reductions in supply chain methane emissions in the Permian, blue hydrogen will not be a low-carbon hydrogen production pathway.

Counterfactuals dictate relative advantages of blue hydrogen over other methods of producing hydrogen. In the Marcellus basin, blue hydrogen has a significantly lower lifecycle GHG emissions intensity compared to grid-based electrolysis given that coal is a significant source of electricity. As recent work suggests, electrolysis – with its high energy requirements – is only low carbon under strict conditions of hourly matching and clean energy additionality. In a world where hydrogen demand is high, the choice of production pathway should be based on a localized and relative analysis of available deployment options. In some regions such as the Marcellus where abundant and low-emission natural gas is readily available, blue hydrogen could be a viable pathway, while regions in the Southwest with abundant solar potential would be better served with hourly matched electrolysis-based hydrogen production. Finally, blue hydrogen could be a viable alternative only in natural gas producing regions where infrastructure is already in place and if the

life cycle GHG emissions are lower than other technologies. Given long infrastructure timelines associated with pipelines and other natural gas infrastructure, pathways that rely on clean electricity may present a faster option for low-carbon hydrogen production in regions that do not have existing natural gas infrastructure.

Limitations of this study have been discussed throughout this analysis. In addition, we conclude by emphasizing the need for continued updates to analyses of the GHG emissions intensity of blue hydrogen projects. Methane emissions from the oil and gas supply chain will rapidly decline because of several factors over the next decade – state and federal regulations, methane fees in the Inflation Reduction Act, voluntary monitoring, reporting, and verification (MRV) initiatives, and growing interest from investors, insurance firms, and civil society. With rapid developments in emissions monitoring technology, it is imperative to develop timely, transparent, and measurement-based estimates of supply chain methane emissions to continually evaluate the GHG intensity of blue hydrogen relative to other production pathways. Blue hydrogen facilities that may not be eligible for the PTC today may become eligible tomorrow if reductions in supply chain methane emissions can be credibly verified.

Methods

Key assumptions

The analysis of blue hydrogen GHG life cycle assessment (LCA) presented here incorporates measurement-informed methane emissions across the natural gas supply chain. Aggregating data across all publicly available emissions estimates, we calculate a production through transmission methane emission rate of 1.25% for the Marcellus basin and 4.95% for the Permian Basin. These are explained in greater detail below and further in the SI. Furthermore, the base case blue hydrogen supply chain considers a carbon capture rate of 96.2% with two solvent units from Lewis et al.[56]: pre-combustion and post-combustion capture. The pre-combustion carbon capture achieved by methyl diethanolamine (MDEA) captures CO_2 from the by-product generated by the SMR reaction, while the post-combustion capture accomplished using Shell's Cansolv solvent absorbs the CO_2 generated by fuel combustion. As a result, the overall carbon capture efficiency increases by implementing these two absorption processes. Transmission compressor stations are assumed to be operated using reciprocating engines since approximately 78% of the compressors in the U.S. are the reciprocating type[57].

Emissions Allocation

Conventional LCA protocols as defined by ISO 14040 rule require emissions allocation among different co-products when there is more than one output flow[58]. We use a bulk, energy-based and product-assigned allocation method, which allows for consideration of the different streams produced in each facility type[59–61]. In the Permian basin, emissions are allocated between crude oil and produced gas in the production stage – these values are typically reported at the facility level to relevant state and federal regulatory agencies. The produced gas is a high-pressure fluid mixture that contains natural gas and natural gas liquids (NGLs). However, NGLs are only separated at the processing stage. Thus, a second emissions allocation is done at the processing stage between dry natural gas used for hydrogen production and NGLs. Similarly, although no crude oil is produced in the Marcellus shale basin, emissions are allocated between dry natural gas and NGLs at the processing stage. Table S3 summarizes the proportion of GHG emissions allocated to different products in each stage of the hydrogen supply chain.

Incorporating top-down methane measurements into LCA framework

Methane emissions across the natural gas supply chain is estimated based on data from publicly available peer-reviewed studies. Across all stages, top-down methane emissions measurements such as those obtained using aerial surveys or satellites is used to estimate measurement-informed emissions inventory for each stage. For the production and gathering and boosting stage of the supply chain, data from top-down aerial field campaigns and satellites are aggregated and averaged to generate a production-normalized methane emission rate for each basin. Data for processing and transmission stages are obtained from a combination of facility-specific operational data and top-down measurement field campaigns. In all measurement-informed inventory estimates, emissions below the detection threshold of the measurement instrument were included when the original studies only report on measured emissions. Detailed estimates are provided below where each supply chain stage is discussed individually. Additional information is provided in the SI. Tables S3 and S4 show the estimated methane emissions using data from these studies.

Blue Hydrogen Life cycle assessment (LCA)

We develop a model for a well-to-gate life cycle assessment (LCA) for blue hydrogen with system boundaries that include drilling and completion of a well through the capture, compression, and injection of CO_2 in the subsurface. This assessment excludes emissions associated with hydrogen transportation to the end user and assumes that the hydrogen production facility is located near demand centers and will not require extensive hydrogen transportation networks. This assumption enables our results to serve as a benchmark for the 45V PTC since the foundation for the tax credit provisions is a well-to-gate LCA that excludes emissions from hydrogen transportation and use. Thus, potential GHG impacts from hydrogen leakage are neglected in this study. The functional unit of our LCA is 1 kg H_2 – all mass units are converted to energy units using higher heating values (HHV) to track various co-products across the supply chain. LCAs are informed by a Life Cycle Inventory (LCI) conducted in accordance with standard ISO guidelines for life cycle assessments[58]. Detailed information on supply chain emissions inventory and all relevant equations are available in methods and the Supplementary Information (SI section S11).

Emissions across different stages of the supply chain are estimated through a detailed life cycle inventory (LCI) that considers all material and energy inputs to each stage. Both the flow of fuels and emissions are tracked throughout the supply chain including (1) CO_2 emissions resulting from the combustion of fuels including natural gas and diesel, (2) CH_4 emissions from the natural gas supply chain, and (3) emissions associated with the electric grid used to power SMR and carbon capture and storage. The following sections describe key data sources and assumptions associated with estimating CO_2 and CH_4 emissions at each stage of the LCA. Each section also describes differences in assumptions and data sources between the Marcellus and Permian supply chains.

Drilling and completions

Methane emissions associated with drilling were estimated from a top-down aerial survey in southwestern Pennsylvania, which determined a methane mass flow rate of 34 g/s per well from a well pad in the drilling phase, occurring for an average of 22 days of drilling efficiency of typical unconventional wells[62]. During well completion, a mixture of reservoir gas, water and slick water with proppant flows back to the surface to a separator, after which natural gas is sent to a flare with an assumed 98% destruction efficiency, and to open tanks, where it is vented. These volumes of vented gas are considered in our analysis based on direct source methane measurements with an infrared camera done specifically for well completion flowbacks in the Appalachian and Gulf Coast regions by Allen et al[63].

Diesel is used for drilling and fracking, which releases CO_2 into the atmosphere during combustion. The LCI for this process is informed by the operational parameters presented in Mallapragada et al.[64] for the Marcellus basin. No public data were found for fuel use to drill and fracture a well in the Permian basin, so parameters for fuel use from the Bakken and the same operator were used to account for these emissions[65]. The use of data from the Bakken shale basin as a proxy for the Permian basin drilling is justified because the fuel for drilling is a function of the well's total depth. The average total depth of 14,628 ft for unconventional wells in the Bakken shale (Williston basin) is comparable to the average total depth for unconventional wells in the

Permian basin of 12,177 ft[66]. On the other hand, the average total well depth in the Appalachian basin, where the Marcellus is located, is 7,947 ft[66].

Production and gathering & boosting

Once the well has been completed, it enters the production stage. Here, produced oil is gathered within a pipeline network to be sent to refineries and natural gas is compressed and transported to gas processing plants. The analysis for the Marcellus shale is based on the southwestern region, which is known for producing wet gas. In contrast, most of the Permian basin produces oil and associated gas with a gas-oil-ratio (GOR) less than 4,000 scf/bbl[67]. This means that for the production stage all the emissions in the Marcellus shale correspond to produced natural gas (dry natural gas and natural gas liquids), while the emissions in the Permian basin must be allocated between crude oil and produced natural gas. The energy flows at this stage include (1) fuel consumption and (2) gas loss or emissions due to methane leakage, liquids unloading and flaring.

In oil and gas facilities, a percentage of natural gas that flows through a facility is used as fuel to power gas-driven equipment. For production and gathering and boosting facilities in the Marcellus, this percentage is estimated to be 2.32% unit volume of fuel gas per unit volume of throughput based on field data from Mallapragada et al[64]. For the Permian basin, this ratio is estimated to be 5.02%, according to Roman-White et al[39]. The higher fraction of natural gas used in operations in the Permian is a result of the lesser degree of electrification compared to the Marcellus basin.

CO_2 emissions from fuel combustion is given by:

$$CO_{2\,fuel\ combustion} = \ Fuel\ use \cdot m_{gas\ throughput} \cdot \ CO_2\ emission\ factor$$

Where:
$Fuel\ use$ = Percentage of gas throughput used as fuel (unit volume fuel gas/unit volume throughput - %)
$m_{gas\ throughput}$ = Mass of gas throughput (kg)
$CO_2\ emission\ factor$ = kg CO_2 emitted per kg NG burned (2.69 kg CO_2/kg NG)

Measurement-informed methane emissions was calculated by aggregating data from peer-reviewed studies that conducted top-down methane measurements (aerial surveys and satellite-based observations). These estimates were then converted it into production normalized emission rate in the Marcellus and Permian basin (SI tables S3 and S4). Methane emissions for each LCA stage is given by:

$$CH_4\ emissions = Avg\ CH_4\ emission\ rate \cdot m_{gas} \cdot \chi_{CH4} \cdot GWP \qquad (1)$$

Where:
$Avg\ CH_4\ emission\ rate$ = Average production-normalized methane emissions rate (%)
m_{gas} = Mass of gas required per stage to produce 1 kg H_2 (kg)

χ_{CH4} = Mass fraction of methane in raw natural gas (for production and processing) and pipeline quality gas (for transmission and SMR)
GWP = Global Warming Potential (kg CO_2e/kg CH_4)

Gas composition varies depending on the supply chain stage. Tables S6 and S7 show the gas composition of produced gas in the Permian and Marcellus basin, respectively[64,68].

Liquids unloading was also considered as an intermittent source of methane emissions. Not all wells require liquid unloading during their lifetime or have unloading that cause emissions. Furthermore, only wells with non-plunger systems result in methane emissions being vented to the atmosphere. As a reference, only 13% of gas wells in the U.S. in 2012 vented gas resulting in emissions from liquids unloading[69]. For this study, one liquid unloading event with emissions per well is considered. Data from liquid unloading in the Appalachian and Permian basins from Zaimes et al.[66] was used to estimate emissions associated with liquid unloading.

Producing wells often flare some volume of gas when the fields do not have the necessary infrastructure to further process gas. We assume a flare destruction efficiency of 98%, following EPA guidelines for well operated flares. Direct measurements of flare destruction efficiency by Caulton et al.[70], where the authors sampled flares in Pennsylvania and North Dakota with an airborne sensor, concluded that all the flares functioned with an efficiency of >99.8%. These emissions are embedded in the top-down methane measurements previously mentioned in the main text and are not considered separately in the LCI to avoid double counting. However, CO_2 emissions from flares are included separately as field campaigns only measure methane emissions. Data from the satellite-informed tool SkyTruth[71] shows that the volume of gas flared in the Permian is higher than that being flared in the Marcellus. In addition, no publicly available data was found regarding how much volume of gas is flared from wells in routine production – recent studies indicate that flare volumes depend on several basin-specific factors such as pipeline takeaway capacity, price of natural gas and crude oil, and demand[72]. Only Marcellus data for flaring during well completions was found and these emissions were included in the previous section. Furthermore, a recent analysis by Rystad Energy and the Environmental Defense Fund[73] concluded that flaring intensity in the Permian is about 1%.

Natural gas processing

Gas processing allows for the separation of produced gas into two product streams: natural gas liquids (NGLs) and dry natural gas. The energy allocation for this stage is achieved based on the NGL yield for each region, which is the ratio of barrels of NGL to the volume of produced natural gas. The Energy Information Administration (EIA)[74] reported that the Northern Appalachian basin, where the Marcellus shale is located, has a NGL yield of 72 bbl/MMscf on average, whereas the Permian basin generates a higher yield of 95 bbl/MMscf due to the larger percentage of heavier hydrocarbons. During processing, energy from NG flows as (1) produced gas condensed to NGL, (2) fuel consumption, and (3) gas loss or emissions due to methane leakage.

The fuel consumption ratio for the Marcellus and Permian basin is estimated to be 0.19% and 2.3%, respectively, based on available data from the literature[64,68,75]. The only source of methane emissions in this stage is from the methane leakage from equipment. Tables S3 and S4 provide details about the data used to estimate an average methane leakage rate. Gas compositions

are obtained from Mallapragada et al.[64] and Contreras et al.[68] for the Marcellus and Permian basins, respectively.

Natural gas transmission

Since the transmission network only transports natural gas with specific quality requirements, all emissions correspond to natural gas only and there is no emissions allocation in this stage. The energy flows in this stage include (1) fuel for compressors and (2) gas loss or emissions due to methane leakage.

The compressors in this study are assumed to be gas-driven reciprocating engines. Approximately 78% of compressors in the U.S. are reciprocating engines, 19% are centrifugal engines and 3% are electrical centrifugal engines[57]. Fuel consumption is directly proportional on the number of compression stations as volumes are assumed to be constant for a steady state blue hydrogen production. Furthermore, the number of compressor stations is a function of the transmission distance from the gas producing region to the demand point. For the Marcellus shale, the demand center is assumed be located in Ohio[76]. For the Permian basin, Houston is likely to have demand for hydrogen in the short or medium term. For this analysis, an average of one compressor station is considered to transport gas from the southwest Marcellus shale to Ohio and five compressor stations to transport gas from the Permian basin to Houston (SI section Sx). The number of compressor stations was estimated based on the assumption that the average distance between transmission compressor stations in the US is about 75 miles[57] and direct mapping of individual stations from the Homeland Infrastructure Foundation-Level Data (HIFLD). The energy associated with fuel required for operating compressor stations is given by:

$$E_{fuel} = \frac{42.418 \cdot 60 \cdot p \cdot t_{op}}{\eta} \cdot n_{units} \cdot n_{stations} \quad (2)$$

Where:
E_{fuel} = Energy required from fuel for each compressor station (BTU/yr)
p = reciprocating engine power (hp)
η = reciprocating engine efficiency (dimensionless)
t_{op} = operating hours (hrs/year)
n_{units} = number of compressor units per compressor station
$n_{stations}$ = number of compressor stations

Compressor stations also emit methane emissions through methane slip from the engines and other fugitive and vented emissions. The same top-down studies that conducted methane measurements for the production and processing stages also included measurements from select compressor stations. In addition, Zimmerle et al.[77] estimated a mean production-normalized gas leakage of 0.22% for transmission compression stations with reciprocating engines. We aggregate data from all publicly available studies on methane emissions from compressor stations, and account for emissions from pipeline leaks and venting, which is 0.03% of gas throughput[77].

Hydrogen production via SMR with CO_2 capture and compression

The technology for hydrogen production included in this study is Steam Methane Reforming due to its efficiency, economic viability, and commercial readiness. There are two chemical reactions that govern this process:

1) SMR reaction: $CH_4 + H_2O \rightarrow 3H_2 + CO$
2) Water-gas shift (WGS) reaction: $CO + H_2O \rightarrow H_2 + CO_2$

This LCA includes the capture and compression of (1) the CO_2 by-product generated by the SMR reaction and (2) the CO2 generated from fuel combustion. Lewis et al.[56] modeled the flows of feedstocks and fuels for the SMR process with CO_2 capture at each stage. The authors used the Aspen Plus modeling platform to simulate the mass and energy flows for different hydrogen plant designs on a steady-state basis. The plant configuration utilized in our work is an SMR plant with both pre-combustion and post-combustion CO_2 capture. HHV of hydrogen is used to calculate the energy required to produce 1 kg H_2 because the efficiency for SMR used for this analysis is equal to 72.1% on an HHV basis[56]. Two solvent systems are needed to accomplish both types of capture in the same plant. Pre-combustion capture absorbs the CO_2 generated as a by-product from the SMR reactions, while post-combustion capture absorbs the CO_2 generated from the combustion of the natural gas that is used as a fuel to power SMR operations. Methyl diethanolamine (MDEA) is used for the pre-combustion CO_2 capture, which is located before the final stage of SMR (pressure swing adsorption). The syngas from the steam reformer flows through the MDEA column, where CO_2 is absorbed. On the other hand, the post-combustion capture uses Shell's Cansolv solvent, which removes CO_2 from the reformer heater stack, and reduces the CO_2 emitted from the combustion of the natural gas used as a fuel. The previously mentioned operational parameters assume an overall carbon capture efficiency of 96.2% following both pre-combustion and post-combustion capture.

Based on the following equations from McCollum and Ogden[78] the power required to compress CO_2 in its gaseous form and pump it when it reaches a supercritical state at approximately 7.38 MPa, is estimated. Table SX in the SI shows typical CO_2 compressibility and ratio of specific heats for each compression state.

$$W_{s,i} = \left(\frac{1000}{24 \cdot 3600}\right)\left(\frac{m\, Z_s R\, T_{in}}{M\, \eta_{is}}\right)\left(\frac{k_s}{k_s - 1}\right)\left[(CR)^{\frac{k_s}{k_s - 1}} - 1\right] \quad (3)$$

$$W_{s,total} = W_{s,1} + W_{s,2} + W_{s,3} + W_{s,4} + W_{s,5} \quad (4)$$

$$W_p = \left(\frac{1000 \cdot 10}{24 \cdot 36}\right)\left(\frac{m\, (P_{final} - P_{cut-off})}{\rho\, \eta_p}\right) \quad (5)$$

Where:
$W_{s,i}$ = Compression power requirement for each individual stage (kW)
m = CO_2 mass flow rate to be transported to injection site (tonnes/day)
Z_s = Average CO_2 compressibility for each individual stage (dimensionless)
R = Gas constant (kJ/kmol-K)
T_{in} = CO_2 temperature at compressor inlet (K)

M = Molecular weight of CO_2 (kg/kmol)
η_{is} = Isentropic efficiency of compressor (dimensionless)
k_s = Average ratio of specific heats of CO2 for each individual stage Cp/Cv (dimensionless)
CR = Compression ratio of each stage (dimensionless)
$W_{s,total}$ = Total combined compression power requirement for all stages (kW)
P_{final} = Final pressure of CO_2 for pipeline transport (MPa)
$P_{cut-off}$ = Pressure at which compression changes to pumping (MPa)
ρ = Density of CO_2 during pumping (kg/m3)
η_p = Efficiency of pump (dimensionless)

The total power requirement for a plant configuration of SMR with CO_2 capture and compression integrated as described above is 26,893.6 kW or 1.34 kWh/kg H_2. The power required for SMR and CO_2 capture was obtained from Lewis et al.[56] and the power requirement for CO_2 compression and pumping for supercritical CO_2 was calculated using equations 3 – 5. The normalized SMR power is 0.35 kWh/kg H_2, which is 26% of the total power and for CO_2 handling (i.e., both capture and compression) is 0.98 kWh/kg H_2, equal to 74% of the total power.

Emissions from the electric grid vary for different supply chains based on the location of the SMR facility. According to the latest data from the Emissions & Generation Resource Integrated Database (eGRID) from the Environmental Protection Agency (EPA), the state of Texas has an average electricity emissions factor of 0.39 kg CO_2e/kWh, whereas Ohio has electric grid emissions factor of 0.55 kg CO_2e/kWh.

CO_2 transportation and injection

We also estimated the pipeline distance from the CO_2 capture and compression facility to the closest CO_2 injection well with ArcGIS. However, the exact location of CO_2 pipelines was not available for the locations in our study, so the calculated distance is based on the location of the available CO_2 injection wells. The power requirement to pump CO_2 through this distance and the power required to inject CO_2 based on injection pressure needed are calculated based on equation 5. An estimate of the injection pressure is based on the normal pressure gradient of 0.433 psi/ft and the depth of the candidate formations for CO_2 storage for each case[79,80].

The supercritical CO_2 must be pumped to the CO_2 injection site. The estimated pressure drop along CO_2 pipelines is 0.13 MPa/mile, according to NETL. The CO_2 pressure at the injection site is given by:

$$P_{CO2} = P_{final} - (\Delta P_{drop} \cdot d) \qquad (6)$$

Where:
P_{CO2} = CO_2 pressure at injection site (MPa)
P_{final} = Final CO_2 pressure after pumping (MPa)
ΔP_{drop} = Pressure drop along CO_2 transportation pipeline (MPa/mile)
d = Distance between the hydrogen plant and the CO_2 injection site (miles)

An estimate of the injection pressure assuming a normal hydrostatic pressure gradient of 0.433 psi/ft and an average depth of formations for CO_2 sequestration based on the literature[79,80] can be determined by:

$$P_{inj} = \frac{1}{145} \cdot \Delta P_g \cdot D \qquad (7)$$

Where:
P_{inj} = Injection pressure (MPa)
ΔP_g = Normal hydrostatic pressure gradient (0.433 psi/ft)
D = Depth of formation for CO_2 sequestration (ft)

References

1. van Renssen, S. The hydrogen solution? *Nat. Clim. Change* **10**, 799–801 (2020).
2. International Energy Agency. *Global Hydrogen Review 2023*. https://www.iea.org/reports/global-hydrogen-review-2023 (2023).
3. European Commission, Directorate-General for Communication (European Commission). *The role of hydrogen in meeting our 2030 climate and energy targets*. https://data.europa.eu/doi/10.2775/833 (2021).
4. Adler, E. J. & Martins, J. R. R. A. Hydrogen-powered aircraft: Fundamental concepts, key technologies, and environmental impacts. *Prog. Aerosp. Sci.* **141**, 100922 (2023).
5. Hoang, A. T. *et al.* Technological solutions for boosting hydrogen role in decarbonization strategies and net-zero goals of world shipping: Challenges and perspectives. *Renew. Sustain. Energy Rev.* **188**, 113790 (2023).
6. Griffiths, S., Sovacool, B. K., Kim, J., Bazilian, M. & Uratani, J. M. Industrial decarbonization via hydrogen: A critical and systematic review of developments, socio-technical systems and policy options. *Energy Res. Soc. Sci.* **80**, 102208 (2021).
7. Sepulveda, N. A., Jenkins, J. D., Edington, A., Mallapragada, D. S. & Lester, R. K. The design space for long-duration energy storage in decarbonized power systems. *Nat. Energy* **6**, 506–516 (2021).
8. The White House. Biden-Harris Administration Announces $7 Billion For America's First Clean Hydrogen Hubs, Driving Clean Manufacturing and Delivering New Economic Opportunities Nationwide. *Energy.gov* (2023).
9. United Kindgom Department for Energy Security and Net Zero. *Hydrogen net zero investment roadmap*. https://www.gov.uk/government/publications/hydrogen-net-zero-investment-roadmap (2023).
10. European Commission. Commission approves up to €5.2 billion of public support by thirteen Member States for the second Important Project of Common European Interest in the hydrogen value chain. *European Commission - European Commission* (2022).
11. Hydrogen. https://www.irena.org/Energy-Transition/Technology/Hydrogen (2023).
12. Spek, M. van der *et al.* Perspective on the hydrogen economy as a pathway to reach net-zero CO 2 emissions in Europe. *Energy Environ. Sci.* **15**, 1034–1077 (2022).
13. Odenweller, A., Ueckerdt, F., Nemet, G. F., Jensterle, M. & Luderer, G. Probabilistic feasibility space of scaling up green hydrogen supply. *Nat. Energy* **7**, 854–865 (2022).
14. Yang, X., Nielsen, C. P., Song, S. & McElroy, M. B. Breaking the hard-to-abate bottleneck in China's path to carbon neutrality with clean hydrogen. *Nat. Energy* **7**, 955–965 (2022).
15. Davis, S. J. *et al.* Net-zero emissions energy systems. *Science* **360**, eaas9793 (2018).
16. Bauer, C. *et al.* On the climate impacts of blue hydrogen production. *Sustain. Energy Fuels* **6**, 66–75 (2021).
17. Oni, A. O., Anaya, K., Giwa, T., Di Lullo, G. & Kumar, A. Comparative assessment of blue hydrogen from steam methane reforming, autothermal reforming, and natural gas decomposition technologies for natural gas-producing regions. *Energy Convers. Manag.* **254**, 115245 (2022).

18. Lewis, E. *et al. Comparison of Commercial, State-of-the-Art, Fossil-Based Hydrogen Production Technologies*. DOE/NETL-2022/3241, 1862910 https://www.osti.gov/servlets/purl/1862910/ (2022) doi:10.2172/1862910.
19. Terlouw, T., Bauer, C., McKenna, R. & Mazzotti, M. Large-scale hydrogen production via water electrolysis: a techno-economic and environmental assessment. *Energy Environ. Sci.* **15**, 3583–3602 (2022).
20. *Inflation Reduction Act of 2022*. *USC* (2022).
21. Argonne National Lab. *The Greenhouse gases, Regulated Emissions, and Energy use in Technologies Model*. https://greet.anl.gov/ (2017).
22. Howarth, R. W. & Jacobson, M. Z. How green is blue hydrogen? *Energy Sci. Eng.* **9**, 1676–1687 (2021).
23. Sánchez-Bastardo, N., Schlögl, R. & Ruland, H. Methane Pyrolysis for Zero-Emission Hydrogen Production: A Potential Bridge Technology from Fossil Fuels to a Renewable and Sustainable Hydrogen Economy. *Ind. Eng. Chem. Res.* **60**, 11855–11881 (2021).
24. Ricks, W., Xu, Q. & Jenkins, J. D. Minimizing emissions from grid-based hydrogen production in the United States. *Environ. Res. Lett.* **18**, 014025 (2023).
25. Alvarez, R. A. *et al.* Assessment of methane emissions from the U.S. oil and gas supply chain. *Science* eaar7204 (2018) doi:10.1126/science.aar7204.
26. Chan, E. *et al.* Eight-Year Estimates of Methane Emissions from Oil and Gas Operations in Western Canada Are Nearly Twice Those Reported in Inventories. *Environ. Sci. Technol.* **54**, 14899–14909 (2020).
27. Shen, L. *et al.* Satellite quantification of oil and natural gas methane emissions in the US and Canada including contributions from individual basins. *Atmospheric Chem. Phys. Discuss.* 1–22 (2022) doi:10.5194/acp-2022-155.
28. Wang, J. L. *et al.* Multiscale Methane Measurements at Oil and Gas Facilities Reveal Necessary Frameworks for Improved Emissions Accounting. *Environ. Sci. Technol.* (2022) doi:10.1021/acs.est.2c06211.
29. Daniels, W. S. *et al.* Toward Multiscale Measurement-Informed Methane Inventories: Reconciling Bottom-Up Site-Level Inventories with Top-Down Measurements Using Continuous Monitoring Systems. *Environ. Sci. Technol.* **57**, 11823–11833 (2023).
30. Lauvaux, T. *et al.* Global assessment of oil and gas methane ultra-emitters. *Science* **375**, 557–561 (2022).
31. Conrad, B., Tyner, D., Li, H., Xie, D. & Johnson, M. Measurement-Based Methane Inventory for Upstream Oil and Gas Production in Alberta, Canada Reveals Higher Emissions and Starkly Different Sources than Official Estimates. Preprint at https://doi.org/10.21203/rs.3.rs-2743912/v1 (2023).
32. Chen, Y. *et al.* Quantifying Regional Methane Emissions in the New Mexico Permian Basin with a Comprehensive Aerial Survey. *Environ. Sci. Technol.* **56**, 4317–4323 (2022).
33. Cusworth, D. H. *et al.* Intermittency of Large Methane Emitters in the Permian Basin. *Environ. Sci. Technol. Lett.* acs.estlett.1c00173 (2021) doi:10.1021/acs.estlett.1c00173.
34. Robertson, A. M. *et al.* New Mexico Permian Basin Measured Well Pad Methane Emissions Are a Factor of 5–9 Times Higher Than U.S. EPA Estimates. *Environ. Sci. Technol.* (2020) doi:10.1021/acs.est.0c02927.

35. Omara, M. *et al.* Methane Emissions from Conventional and Unconventional Natural Gas Production Sites in the Marcellus Shale Basin. *Environ. Sci. Technol.* **50**, 2099–2107 (2016).
36. Barkley, Z. *et al.* Quantification of oil and gas methane emissions in the Delaware and Marcellus basins using a network of continuous tower-based measurements. *Atmospheric Chem. Phys.* **23**, 6127–6144 (2023).
37. Ren, X. *et al.* Methane Emissions from the Marcellus Shale in Southwestern Pennsylvania and Northern West Virginia Based on Airborne Measurements. *J. Geophys. Res. Atmospheres* **124**, 1862–1878 (2019).
38. Rutherford, J. *et al. Closing the gap: Explaining persistent underestimation by US oil and natural gas production-segment methane inventories*. http://eartharxiv.org/repository/view/1793/ (2020) doi:10.31223/X5JC7T.
39. Roman-White, S. A. *et al.* LNG Supply Chains: A Supplier-Specific Life-Cycle Assessment for Improved Emission Accounting. *ACS Sustain. Chem. Eng.* **9**, 10857–10867 (2021).
40. Gilbert, A. Q. & Sovacool, B. K. Carbon pathways in the global gas market: An attributional lifecycle assessment of the climate impacts of liquefied natural gas exports from the United States to Asia. *Energy Policy* **120**, 635–643 (2018).
41. Nie, Y. *et al.* Greenhouse-gas emissions of Canadian liquefied natural gas for use in China: Comparison and synthesis of three independent life cycle assessments. *J. Clean. Prod.* **258**, 120701 (2020).
42. Jordaan, S. M. *et al.* Global mitigation opportunities for the life cycle of natural gas-fired power. *Nat. Clim. Change* **12**, 1059–1067 (2022).
43. Johnson, M. R., Conrad, B. M. & Tyner, D. R. Creating measurement-based oil and gas sector methane inventories using source-resolved aerial surveys. *Commun. Earth Environ.* **4**, 1–9 (2023).
44. Ravikumar, A. P. *et al.* Measurement-based differentiation of low-emission global natural gas supply chains. *Nat. Energy* 1–3 (2023) doi:10.1038/s41560-023-01381-x.
45. Sand, M. *et al.* A multi-model assessment of the Global Warming Potential of hydrogen. *Commun. Earth Environ.* **4**, 1–12 (2023).
46. Ocko, I. B. & Hamburg, S. P. Climate consequences of hydrogen emissions. *Atmospheric Chem. Phys.* **22**, 9349–9368 (2022).
47. Ozbilen, A., Dincer, I. & Rosen, M. A. Comparative environmental impact and efficiency assessment of selected hydrogen production methods. *Environ. Impact Assess. Rev.* **42**, 1–9 (2013).
48. Kleijne, K. de, Coninck, H. de, Zelm, R. van, J. Huijbregts, M. A. & V. Hanssen, S. The many greenhouse gas footprints of green hydrogen. *Sustain. Energy Fuels* **6**, 4383–4387 (2022).
49. Energy Transitions Commission. *Making the Hydrogen Economy Possible: Accelerating Clean Hydrogen in an Electrified Economy*. https://www.energy-transitions.org/publications/making-clean-hydrogen-possible/ (2021).
50. Ajanovic, A., Sayer, M. & Haas, R. The economics and the environmental benignity of different colors of hydrogen. *Int. J. Hydrog. Energy* **47**, 24136–24154 (2022).
51. Howarth, R. W. & Jacobson, M. Z. How green is blue hydrogen? *Energy Sci. Eng.* **9**, 1676–1687 (2021).
52. Machhammer, O., Bode, A. & Hormuth, W. Financial and Ecological Evaluation of Hydrogen Production Processes on Large Scale. *Chem. Eng. Technol.* **39**, 1185–1193 (2016).

53. Sánchez-Bastardo, N., Schlögl, R. & Ruland, H. Methane Pyrolysis for Zero-Emission Hydrogen Production: A Potential Bridge Technology from Fossil Fuels to a Renewable and Sustainable Hydrogen Economy. *Ind. Eng. Chem. Res.* **60**, 11855–11881 (2021).
54. Pettersen, J. *et al.* Blue hydrogen must be done properly. *Energy Sci. Eng.* **10**, 3220–3236 (2022).
55. Cheng, F., Luo, H., Jenkins, J. D. & Larson, E. D. Impacts of the Inflation Reduction Act on the Economics of Clean Hydrogen and Synthetic Liquid Fuels. *Environ. Sci. Technol.* **57**, 15336–15347 (2023).
56. Lewis, E. *et al. Comparison of Commercial, State-of-the-Art, Fossil-Based Hydrogen Production Technologies*. https://www.osti.gov/biblio/1862910 (2022) doi:10.2172/1862910.
57. Skone, T. J., Littlefield, J. & Marriott, J. *Life Cycle Greenhouse Gas Inventory of Natural Gas Extraction, Delivery and Electricity Production*. https://www.osti.gov/biblio/1515238 (2011) doi:10.2172/1515238.
58. International Organization for Standardization. ISO 14040:2006, Environmental management — Life cycle assessment — Principles and framework. (2006).
59. Zavala-Araiza, D., Allen, D. T., Harrison, M., George, F. C. & Jersey, G. R. Allocating Methane Emissions to Natural Gas and Oil Production from Shale Formations. *ACS Sustain. Chem. Eng.* **3**, 492–498 (2015).
60. Aldrich, R., Llauró, F. X., Puig, J., Mutjé, P. & Pèlach, M. À. Allocation of GHG emissions in combined heat and power systems: a new proposal for considering inefficiencies of the system. *J. Clean. Prod.* **19**, 1072–1079 (2011).
61. Rosselot, K. S., Allen, D. T. & Ku, A. Y. Comparing Greenhouse Gas Impacts from Domestic Coal and Imported Natural Gas Electricity Generation in China. *ACS Sustain. Chem. Eng.* **9**, 8759–8769 (2021).
62. Caulton, D. R. *et al.* Toward a better understanding and quantification of methane emissions from shale gas development. *Proc. Natl. Acad. Sci.* **111**, 6237–6242 (2014).
63. Allen, D. T. *et al.* Measurements of methane emissions at natural gas production sites in the United States. *Proc. Natl. Acad. Sci.* **110**, 17768–17773 (2013).
64. Mallapragada, D. S. *et al.* Life cycle greenhouse gas emissions and freshwater consumption of liquefied Marcellus shale gas used for international power generation. *J. Clean. Prod.* **205**, 672–680 (2018).
65. Laurenzi, I. J., Bergerson, J. A. & Motazedi, K. Life cycle greenhouse gas emissions and freshwater consumption associated with Bakken tight oil. *Proc. Natl. Acad. Sci.* **113**, E7672–E7680 (2016).
66. Zaimes, G. G. *et al.* Characterizing Regional Methane Emissions from Natural Gas Liquid Unloading. *Environ. Sci. Technol.* **53**, 4619–4629 (2019).
67. Energy Information Administration. Advances in technology led to record new well productivity in the Permian Basin in 2021. https://www.eia.gov/todayinenergy/detail.php?id=54079 (2022).
68. Contreras, W. *et al.* Life cycle greenhouse gas emissions of crude oil and natural gas from the Delaware Basin. *J. Clean. Prod.* **328**, 129530 (2021).
69. Allen, D. T. *et al.* Methane Emissions from Process Equipment at Natural Gas Production Sites in the United States: Liquid Unloadings. *Environ. Sci. Technol.* **49**, 641–648 (2015).

70. Caulton, D. R. *et al.* Methane Destruction Efficiency of Natural Gas Flares Associated with Shale Formation Wells. *Environ. Sci. Technol.* **48**, 9548–9554 (2014).
71. Earth Observation Group. SkyTruth Flaring Map.
72. Lyon, D. R. *et al.* Concurrent variation in oil and gas methane emissions and oil price during the COVID-19 pandemic. *Atmospheric Chem. Phys.* **21**, 6605–6626 (2021).
73. Goldstein, J. & Weatherall, G. New Rystad cost analysis makes case for EPA to end routine flaring in final methane rule. *EDF Blogs* https://blogs.edf.org/energyexchange/2022/02/28/new-rystad-cost-analysis-makes-case-for-epa-to-end-routine-flaring-in-final-methane-rule/ (2022).
74. Energy Information Administration. U.S. natural gas plant liquid production continues to hit record highs. *Today in Energy* https://www.eia.gov/todayinenergy/detail.php?id=38772 (2019).
75. Roman-White, S., Rai, S., Littlefield, J., Cooney, G. & Skone, T. J. *Life cycle greenhouse gas perspective on exporting liquefied natural gas from the Unites States: 2019 update*. https://www.osti.gov/biblio/1607677 (2019) doi:10.2172/1607677.
76. Henning, M., Thomas, A., Psarras, P. & Triozzi, M. *Developing a Hydrogen Economy in Ohio: Challenges and Opportunities*. 1–76 https://engagedscholarship.csuohio.edu/urban_facpub/1765 (2022).
77. Zimmerle, D. J. *et al.* Methane Emissions from the Natural Gas Transmission and Storage System in the United States. *Environ. Sci. Technol.* **49**, 9374–9383 (2015).
78. McCollum, D. L. & Ogden, J. M. *Techno-Economic Models for Carbon Dioxide Compression, Transport, and Storage & Correlations for Estimating Carbon Dioxide Density and Viscosity*. https://escholarship.org/uc/item/1zg00532 (2006).
79. Cumming, L., Hawkins, J., Sminchak, J., Valluri, M. & Gupta, N. Researching candidate sites for a carbon storage complex in the Central Appalachian Basin, USA. *Int. J. Greenh. Gas Control* **88**, 168–181 (2019).
80. Gulf Coast Carbon Center. SACROC Research Project | Gulf Coast Carbon Center. https://gccc.beg.utexas.edu/research/sacroc.

Supplementary Information

Geospatial Variation in Carbon Accounting of Blue Hydrogen Production Pathways: Implications for the Inflation Reduction Act

37 pages, 41 tables, 3 figures

Valeria Vallejo[1], Quoc Nguyen[1], and Arvind P. Ravikumar*[1,2]

[1]Department of Petroleum and Geosystems Engineering, The University of Texas at Austin, Austin, TX USA

[2]Energy Emissions Modeling and Data Lab, The University of Texas at Austin, Austin, TX, USA

*Corresponding author email: arvind.ravikumar@austin.utexas.edu

Table of Contents

S1. Tax credit tiers established by the Inflation Reduction Act

The Inflation Reduction Act (IRA) in the United States includes tax credit provisions for clean hydrogen production[1]. This federal law defines clean hydrogen as "hydrogen which is produced through a process that results in a lifecycle greenhouse gas emissions rate of not greater than 4 kilograms of CO_2e per kilogram of hydrogen". Section 45V of the Inflation Reduction Act presents the criteria shown in Table S1 to determine the percentage of tax credit that an entity can claim when producing clean hydrogen.

Table S1: Production Tax Credit (PTC) applicable percentages and credit amount per kg H_2 based on life cycle GHG emissions intensity.

Life cycle GHG emissions rate (kg CO_2e/kg H_2)	**Applicable percentage (%)**	**Credit amount ($/kg H_2)**
2.50 – 4.00	20.0	0.60
1.50 – 2.50	25.0	0.75
0.45 – 1.50	33.4	1.00
< 0.45	100.0	3.00

S2. Life Cycle Inventory (LCI)

Life cycle assessment (LCA) models are informed by a Life Cycle Inventory (LCI), that represent all inputs necessary to describe energy and material flows through the life cycle and is defined by the International Standards Organization (ISO) 14040 standard[2]. Emissions across different stages of the supply chain are estimated through a detailed life cycle inventory (LCI) that considers all material and energy inputs to each stage. The complete LCI for the case studies presented here can be found section S11.

S3. Geospatial data of natural gas supply chains

The case studies developed in this research are based on the Marcellus shale and the Permian basin because these basins have the highest dry shale gas production in the United States[3], which is the main feedstock for blue hydrogen. Since the scale up of hydraulic fracturing in the 2010s, the U.S. has experienced a rapid growth of shale gas exploitation. Shale gas accounted for 80% of the total dry gas production in the U.S. in 2022, according to the EIA[4].

The Marcellus shale is characterized for being a gas-rich region with two distinct sub-regions – the Northeast Marcellus includes wells that mostly produce dry gas while the Southwest Marcellus includes wells that produce liquids-rich gas. Oil production is negligible in the region, with a few wells producing less than bbl/MMscf [5]. Natural gas facilities in the Marcellus shale and existing hydrogen plants are displayed in Figure S1.

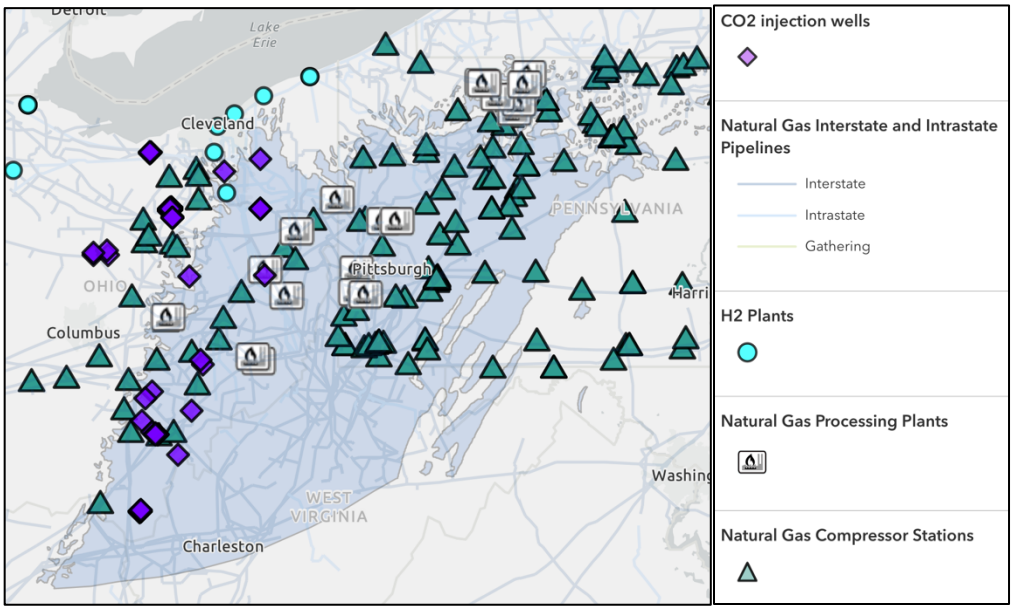

Figure S1. Distribution of facilities in the Marcellus shale and location of H_2 plants in Ohio. Map created in ArcGIS.

Table S2 summarizes the geographic parameters used in the study for the case of blue hydrogen produced with natural gas sourced from Marcellus shale basin.

Table S2. Location and pipeline distance between facilities considered in the Marcellus shale case study.

Type of facility	Latitude	Longitude	Pipeline distance to next facility (mi)	Ref.
Gas processing plant	40.260	-80.260	56.82	[6]
Compressor station	40.825	-80.756	53.04	[7]
H_2 production plant	41.010	-81.610	24.45	[8]
CO_2 injection well	40.900	-81.280		[9]
Distance between gas processing plant and H_2 plant			110	[10]

The Permian basin is located in western Texas and eastern New Mexico, and it is known to be the most prolific gas producing region in the United States. As of 2023, the Permian basin produces approximately 22 Bcf/d of gas and 5.6 MMbbl/d[11]. There are three sub-basins in the Permian: Delaware basin, Midland basin, and Central basin Platform[12]. Most of the wells in this basin produce oil with a GOR below 4,000 scf/bbl and only a small percentage of the wells have a GOR greater than 8,000 scf/bbl[13]. Furthermore, figure S2 shows a current snapshot of the distribution of natural gas assets in the Permian basin and existing hydrogen plants in Houston.

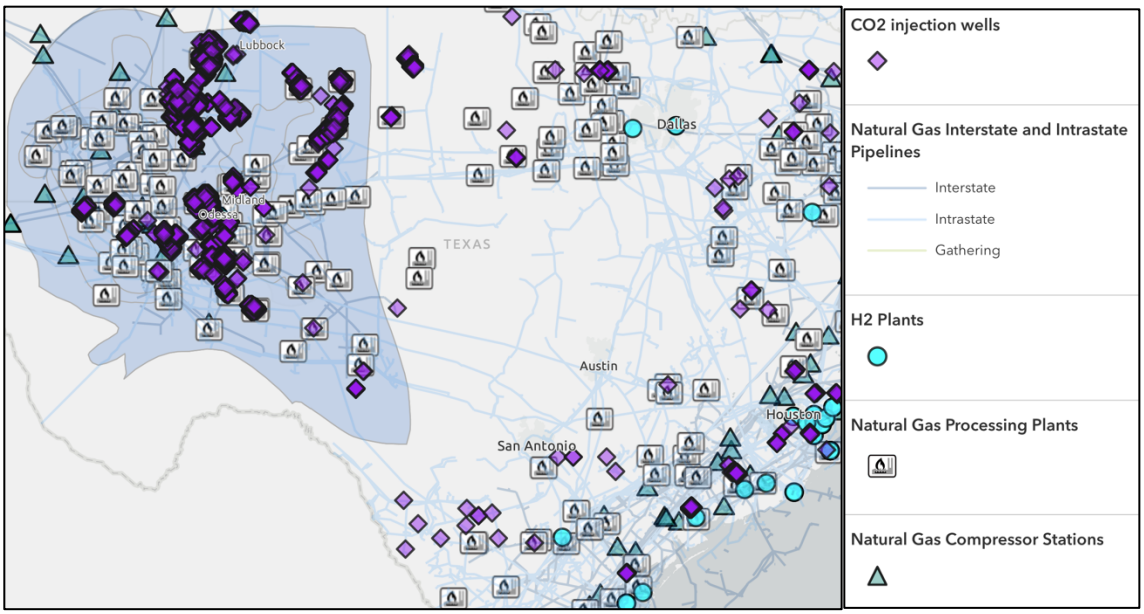

Figure S2. Distribution of facilities in the Permian basin and location of H_2 plants in Houston, TX. Map created in ArcGIS.

Table S3 summarizes the geographic parameters used in the study for the case of blue hydrogen produced with natural gas sourced from the Permian shale basin.

Table S3. Location and pipeline distance between facilities considered in the Permian basin case study.

Type of facility	Latitude	Longitude	Pipeline distance to next facility (mi)	Ref.
Gas processing plant	30.300	-100.650	211.08	6
Compressor station	28.712	-97.675	30.04	7
Compressor station	29.012	-97.146	69.21	7
Compressor station	29.533	-96.144	45.82	7
Compressor station	29.968	-95.485	28.89	7
H_2 production plant	29.760	-95.370	6.85	8
CO_2 injection well	29.650	-95.400		14
Distance between gas processing plant and H_2 plant			385.04	10

S4. Top-down vs. bottom-up approaches to estimate methane emissions

Methane is emitted along different equipment and processes of the natural gas supply chain. Methane emissions can be modeled by two different approaches: top-down (TD) and bottom-up (BU) measurements. TD estimates are taken by airborne systems or satellites at a regional scale in a delimited study area. These measurements are based on atmospheric sampling and the use of atmospheric dispersion or transport models to estimate an emission flux[15]. Aerial surveys fly an aircraft upwind and downwind of the delimited area and then performing a mass balance, i.e., estimating the difference of methane mole fraction among both passes and calculating a mass flow rate of methane. This approach corrects for outside factors such as wind speed and direction[16].

Conversely, BU estimates are calculated by measuring the emission factor of a single equipment and scaling this measurement up by the number of such devices in a specific field or facility, i.e., multiplying an emission factor by an activity factor[16]. This BU approach informs emission inventories[17]. Typically, the emission factors are an average of each type of device; however, this factor needs to accurately represent the behavior of the rest of the equipment population, otherwise, the emissions would be miscalculated. Nevertheless, there are some cases in which the emission factors might not be representative of the population, the activity count might not be up-to-date or both values of emission factors and activity count might be used as an average for a variety of facilities in different locations. All these circumstances can introduce bias to the calculation of methane emissions in a specific facility.

S5. Top-down studies in the Permian basin

Currently, oil and gas operations in the Permian basin have been under scrutiny due to the increase in flaring and venting [18,19] so the TD studies in this area are novel. This work uses the data published by two peer-reviewed papers: Chen et al.[20] and Zhang et al.[18]. These studies are the most

recent in the Permian basin and provide sufficient data to estimate methane emission rates for three LCA stages considered in this research: production, processing, and transmission.

Chen et al.[20] published results of methane emissions from the New Mexico Permian basin. measured by aerial surveys performed by Kairos Aerospace in a 35,923 km^2 area with 26,292 producing wells and 15,000 km of pipelines. The authors also accounted for three important factors: (1) emissions that were below detection threshold, (2) assets not covered in the campaign, and (3) partial detection. The aircraft flew over 90% of the producing wells in multiple occasions from October 2018 to January 2020. The total methane flow derived was 194 tonnes per hour or 9.4% of gross gas production. Additionally, the authors attributed the detected methane plumes to all the facility types surveyed based on proximity to the emitting source, wind direction, and prioritizing localized sources over pipelines. The latter means that if a methane plume is detected near a localized source (i.e., equipment such as compressor station) and a pipeline, the plume is assigned to the localized sources. The study assigns emissions to the following facility types: well sites, gas processing plants, compressor stations, storage tanks, pipeline and "other/ambiguous". Well sites are defined as sites with at least one producing well that have storage tanks, gathering lines, and compressor stations. Thus, well sites are equivalent to production and gathering and boosting from this LCA. Gas processing plants are equivalent to the processing stage. Finally, the definition for compressor stations in the paper does not include any wells or processing plants, only gathering line and storage tanks. Therefore, this category is equivalent to the transmission stage in this LCA. The storage tanks category does not contain any other facility types, only tanks and gathering lines. Kairos did not attribute any plumes to the standalone storage tanks, only to the storage tanks at well sites, processing plants and compressor stations. The pipeline category are pipelines that are 200 m far from any well sites, gas processing plants, compressor stations and storage tanks. Furthermore, the authors explain the number of well sites and gas processing plants

has more certainty than the number of storage tanks and compressor stations because no complete datasets disclosing the number of these type of facilities were found.

For the reasons mentioned above, this research incorporated the emissions contribution from well sites, processing plants and compressor stations but not the standalone storage tanks and pipeline due to the ambiguity of the definitions provided. Also, every facility type incorporated to this research has storage tanks and gathering lines in their definition. Based on the production-normalized emission rate of 9.4%, the emissions contribution from well sites is 52%, from gas processing plants is 2%, and from compressor stations is 17%. It is important to note that the final methane emission rate estimated from this study[20] is higher than that from other peer-reviewed studies [18,21,22].

Zhang et al.[18] derived methane emission rates using Bayesian atmospheric inverse modeling based on a bottom-up inventory extrapolated from EPA as a prior and observations from the spaceborne sensor Tropospheric Monitoring Instrument (TROPOMI) aboard the Copernicus Sentinel-5 Precursor satellite. The satellite measurements were taken from May 2018 to March 2019. The authors estimated methane emissions from oil and gas facilities in the Permian basin to be 2.7 Tg/yr, which is an average emission rate of 3.7% of the gross gas production in the Permian. They also provided information about another emission inventory developed by scaling up ground-based methane measurements in the Permian, which are 2.3 Tg/yr for well sites, 0.14 Tg/yr for gas processing plants, and 0.22 Tg/yr for compressor stations. These estimates were used to disaggregate the 2.7 Tg/yr of methane emissions into the different facility types to estimate the emissions contribution from production, processing, and transmission.

An average emission rate for each facility type is calculated by averaging the mean production-normalized emission rates per facility type. Zhang et al.[18] described the emissions behavior of the Permian as a whole while Chen et al. [20] mostly studied the New Mexico part of the

Permian, so the assumption that the emissions trend in New Mexico is representative of the whole Permian must be made to average these two emission rates as equal. According to Dubey et al. [23], TROPOMI can achieve a detection threshold of approximately 50 kg/h in the Permian basin area for a campaign with a duration of one year, which is the case of the study conducted by Zhang et al.[18]. Only 14% of the 1985 plumes detected by Kairos Aerospace are below 50 kg/h, and these plumes account for approximately 5% of the total methane emission mass rate. This agrees with the heavy-tail distributions characteristic of methane measurements [24,25]. For this reason, this work averages the measurements obtained from both technologies with equal weight since there are not sufficient data available to estimate a weighted average of any sort that does not introduce more bias to the emission rates. The emission rates estimated for each stage (production, processing, and transmission) are presented in Table S4.

Table S4: Top-down methane measurements based on aerial surveys and satellite observations conducted in the Permian basin by peer-reviewed studies. Methane measurements are reported as production-normalized emission rates (%).

Study used to estimate CH_4 emissions	**Methodology**	**Region**	**Mean production-normalized emission rate (%)**
Zhang et al.[18]	TROPOMI measurements disaggregated by stage based on extrapolation of site-level measurements	Permian basin	Production-3.20 Processing-0.19 Transmission-0.31
Chen et al. [20]	Aerial survey by Kairos Aerospace	Permian basin (New Mexico)	Production-4.89 Processing-0.19 Transmission-1.60

S6. Top-down studies in the Marcellus shale

There are similar studies conducted in the Marcellus shale; however, these measurements are not as recent as the surveys in the Permian basin. Our analysis is based on the southwestern

area of Marcellus shale basin because it is closer to the hydrogen demand point. For the Marcellus case, information provided by Caulton et al. [26] and Ren et al. [27] is used.

Caulton et al.[26] conducted an airborne-based study to quantify methane measurements from gas production, processing, transmission, and distribution in southwestern Pennsylvania. This study does not include emissions from the distribution sector because the delivery of natural gas for end use is not part of the hydrogen production chain. The authors reported a low emission rate of 2.8% and a high of 16.4%. Since this study didn't report a mean, a mean is calculated assuming a heavy-tailed distribution, which is characteristic of methane leaks from natural gas systems, according to Brandt et al [24]. Similarly, Frankenberg et al. showed that methane fluxes derived from aerial surveys follow a heavy-tailed distribution[25]. For this reason, this study uses a distribution from one of the studies[24] that measured emissions in production well pads in Southwestern Pennsylvania (Omara et al.[28]) to estimate a mean emission rate of 4.17%. There are inventory-based emission fluxes from facility types of natural gas systems (production, processing, transmission, and distribution). Since [26] reported an emission rate that corresponds to emissions from all the operations related to gas systems, from production to distribution, the previously mentioned inventory values are used to estimate the emissions contribution from production, processing, and transmission. Emissions contribution from distribution is excluded because this is out of the LCA boundary since the delivery of gas to the end user is not a part of this analysis.

Ren et al. [27] followed a similar approach but reported emissions from the distribution sector separately. The authors reported an emission rate of 1.1%, excluding gas distribution, so the same inventory values were used to allocate emissions between production, processing, and transmission facilities. This time the inventory values from distribution are not utilized because this 1.1% emission rate does not include distribution. All the peer-reviewed studies mentioned above developed their own statistical models to estimate methane emissions with a high degree of

accuracy. For both case studies, an average is estimated based on measurements from TD surveys while also accounting for emissions below detection threshold where applicable.

Unlike the studies in the Permian basin, the studies conducted in the Marcellus area do not account for emissions below the detection threshold of the aerial surveys. Different technologies that measure methane emissions have different detection thresholds. The detection threshold is the smallest emission flux that can be detected by a sensor. To account for emissions below this detection threshold, Chen et al.[20] proposed to estimate the percentage of emissions from the national leakage rate that the Kairos sensor would not detect in New Mexico wind conditions. To achieve this, the authors used one of the largest datasets of ground-level measurements performed for 1,009 sites in the U.S. performed by Omara et al[29]. The main finding was that the airborne sensor would only detect emissions in 79 sites. However, these 8% of the 1,009 sites account for around 63% of total emissions from all sites. This phenomenon can be explained with the heavy-tailed distributions of emission sizes that are typical of methane measurements[24,25]. Therefore, they conclude that approximately 37% of ground-level emissions are not detected by the aerial survey and they multiply this proportion by the national average methane leakage obtained from ground-level measurements because they did not have access to any Permian site-level datasets.

Thus, assuming that aerial surveys use similar sensors and have similar detection thresholds, this research applies the same fraction of emissions below the detection threshold of airborne sensors to the site-level measurements. However, in this case there is availability of site-level emissions data specifically for the Marcellus (southwestern Pennsylvania and northern West Virginia) from Omara et al. [28]. This study concluded that a mean of 0.13% is emitted from well pads in routine production. Thus, the 37% of an emission rate of 0.13% is added to the emission rate from the production stage. Table S5 shows the findings and study areas of these studies.

Table S5: Top-down methane measurements based on aerial surveys and satellite observations conducted in the Marcellus shale by peer-reviewed studies. Methane measurements are reported as production-normalized emission rates (%).

Study used to estimate CH_4 emissions	**Methodology**	**Region**	**Mean production-normalized emission rate (%)**
Caulton et al.[26]	Airborne system mass balance	Marcellus shale (Southwestern Pennsylvania)	Production-0.64 Processing-0.10 Transmission-0.72
Ren et al.[27]	Aircraft mass balance	Marcellus shale (Southwestern Pennsylvania and northern West Virginia)	Production-0.70 Processing-0.08 Transmission-0.56

Top-down methane measurements are the best estimates available of methane emission rates in the Marcellus shale and Permian basin. This study uses the most up-to-date top-down studies available in the literature. However, top-down surveys are not ideal because they are a snapshot in time. On one hand, the studies in the Permian basin have a duration of approximately one year, which is sufficient time to capture the temporal variability of emissions. On the other hand, the aerial surveys conducted in the Marcellus shale only last a few days, which might not be enough time to characterize methane emissions from oil and gas facilities. A potential solution to the temporal variation of methane emissions is the use of continuous emissions monitoring systems (CEMS). Nonetheless, there are no peer-reviewed studies that quantify methane emissions in the Marcellus shale and Permian basin. The only known study that uses tower-based continuous monitoring is a preprint by Barkley [30], which estimates production-normalized methane emission rates of 2.5 – 3.5% for the Delaware in the Permian basin and 0.30 – 0.45% for the northeastern Marcellus. The measurements in the Delaware sub-basin were taken from March 2020 to April 2022 and the lowest levels of methane were seen during the COVID-19 pandemic. The measurements in the northeastern Marcellus were taken from May 2015 to December 2016, so

they are not significantly novel than the measurements used in this work. These estimates obtained from CEMS are lower than the average methane emission rates estimated in this research. Finally, when resources to quantify methane emissions are not limited and data availability is not a limitation, a multiscale approach is recommended, where various technologies with different detection thresholds (optical gas imaging cameras, drones, aerial surveys, and satellites) are deployed to quantify methane emissions in a layered manner as proposed by Wang et al.[31] and Esparza et al. [32]. Spatially and temporally resolved quantification of methane measurements can be achieved with the deployment of CEMS and multiscale technologies.

S7. Allocation of GHG emissions

Zavala-Araiza et al.[33] describe a methodology to allocate methane emitted from all the activities related to oil and gas operations to the three products resulting from production and processing, which are crude oil, natural gas, and natural gas liquids. Similarly, Aldrich et al.[34] and GHG Protocol[35] explain the importance of allocating the CO2 emissions resulting from fuel combustion in a facility when there are multiple output streams. Table 5 shows the proportion of GHG emissions allocated to the products in each stage.

In the Permian basin, emissions are allocated between crude oil and produced gas in the production stage. This energy allocation was performed based on the yearly oil and natural gas production obtained from the Railroad Commission of Texas[36]. The produced gas is a high-pressure fluid mixture that consists of natural gas and natural gas liquids. However, natural gas liquids are only separated at the processing stage and are not reported at the production site-level. Thus, a second emissions allocation is done at the processing stage between dry natural gas used for hydrogen production and natural gas liquids. Similarly, although no crude oil is produced in the Marcellus shale basin, emissions are allocated between dry natural gas and natural gas liquids

at the processing stage. The allocation for NGL is calculated based on specific natural gas yields for the Marcellus and Permian obtained from the EIA[37]. The units of NGL yield are bbl/MMcf, which refer to the number of barrels of NGL obtained from 1 MMcf of unprocessed raw gas. Table S5 summarizes the proportion of GHG emissions allocated to different products in each stage of the hydrogen supply chain.

The percentage of emissions corresponding to raw gas and oil resulting from the wellhead is computed as:

$$\%\ emissions\ allocation_{\ oil} = \frac{Q_{\ oil} * E_{\ oil}}{(Q_{\ oil} * E_{\ oil}) + (Q_{\ gas} * E_{\ gas})} \qquad (S1)$$

$$\%\ emissions\ allocation_{\ raw\ gas} = \frac{Q_{\ gas} * E_{\ gas}}{(Q_{\ oil} * E_{\ oil}) + (Q_{\ gas} * E_{\ gas})} \qquad (S2)$$

Where:

$Q_{\ oil}$ = Yearly oil production (bbl/year)

$Q_{\ gas}$ = Yearly gas production (scf/year)

$E_{\ oil}$ = Energy density of oil (5.8 MMBtu/bbl)

$E_{\ gas}$ = Energy density of gas (1172 BTU/scf for Marcellus and 1235 BTU/scf for Permian)*

*Differences due to presence of heavier components in Permian gas.

Subsequently, the fraction of emissions corresponding to natural gas liquids and residue gas originating from the processing plant is estimated as:

$$\%\ emissions\ allocation_{\ NGL} = \frac{NGL\ yield * E_{\ NGL}}{(1\ MMscf * E_{\ gas})} \qquad (S3)$$

$$\%\ emissions\ allocation_{\ residue\ gas} = 1 - \%\ emissions\ allocation_{\ NGL} \qquad (S4)$$

Where:

$NGL\ yield$ = 72 bbl/MMcf for Marcellus and 95 bbl/MMcf for Permian

E_{NGL} = Energy density of natural gas liquids (3.82 MMBtu/bbl)

E_{gas} = Energy density of gas (1172 BTU/scf for Marcellus and 1235 BTU/scf for Permian)

Table S6: Allocation of emissions for each product and stage along the NG supply chain.

Supply chain stage	Product	Share of emissions Marcellus shale	Share of emissions Permian basin
Production	Natural gas	100%	46%
	Crude oil	0%	54%
Processing	Natural gas	77%	71%
	Natural gas liquids	23%	29%

S8. Energy balance

One of the main purposes of this research is to estimate the energy and mass of gas needed to produce 1 kilogram of hydrogen. However, no process is 100% efficient. Additional energy from gas must be accounted for due to the following operational circumstances:

a) Gas loss due to leakage, flaring, and venting, i.e., the aggregate of emissions provided by top-down studies at a basin level and due to liquid unloading.
b) Fuel consumption of gas-driven equipment along the supply chain
c) Efficiency of SMR

To calculate the energy of natural gas needed to produce 1 kg H_2, all the parameters mentioned above need to be accounted for along the natural gas supply chain from gas extraction, which is the gas production stage, to the hydrogen production plant. The starting point is the energy required to produce 1 kg H_2 based on the cold gas efficiency of the SMR plant, which is equal to 72.1% on an HHV basis [38]. The fuel required was calculated based on the Aspen Plus steady state simulation from Lewis et al. [38], where the 15.35% of the natural gas feed flowrate for SMR is used

as a fuel. The amount of mass needed for 1 kg H_2 is equal to the sum of the mass required for 1 kg H_2 and for the fuel.

The energy required from natural gas from the previous supply chain stages (until production) is reverse calculated based on the energy needed for 1 kg H_2. This is essentially an energy balance. Following the law of conservation of energy, this energy balance is repeated until the production stage of the LCA has been reached. Thus, this is the amount of energy needed from natural gas to produce 1 kg H_2 accounting for all gas losses and fuel use. The total energy required from natural gas per stage can be converted to mass based on the heating value and density of natural gas in each stage, which is obtained based on the gas composition of residue and raw gas from the LCI.

S9. Supplementary results

Base Case Scenario

Table S7: Marcellus shale base case – life cycle GHG emissions of blue hydrogen production in Ohio using natural gas derived from the Marcellus shale disaggregated across key life cycle stages. Results expressed in both GWP-100 and GWP-20.

GHG	Drilling and completions	Production	Processing	Transmission	SMR	CCS	Emissions by GHG
CO_2 (kg CO_2/kg H_2)	0.03	0.37	0.02	0.06	0.62	0.57	1.67
CH_4 (kg CH_4/kg H_2)	$5.4x10^{-4}$	0.03	0.003	0.03	-	-	0.06
CH_4 GWP-100 (kg CO_2e/kg H_2)	0.01	0.82	0.08	0.71	-	-	1.62
CH_4 GWP-20 (kg CO_2e/kg H_2)	0.04	2.39	0.23	2.07	-	-	4.73
Total emissions GWP-100 (kg CO_2e/kg H_2)	0.04	1.19	0.10	0.77	0.62	0.57	**3.3**

Total emissions GWP-20 (kg CO_2e/kg H_2)	0.07	2.76	0.25	2.13	0.62	0.57	**6.4**

Table S8: Permian basin base case – life cycle GHG emissions of blue hydrogen production in Houston, TX using natural gas derived from the Permian basin disaggregated across key life cycle stages. Results expressed in both GWP-100 and GWP-20.

GHG	Drilling and completions	Production	Processing	Transmission	SMR	CCS	Emissions by GHG
CO_2 (kg CO_2/kg H_2)	0.02	1.02	0.29	0.21	0.56	0.39	2.49
CH_4 (kg CH_4/kg H_2)	5.88×10^{-4}	0.13	0.004	0.04	-	-	0.17
CH_4 GWP-100 (kg CO_2e/kg H_2)	0.02	3.61	0.12	1.21	-	-	4.96
CH_4 GWP-20 (kg CO_2e/kg H_2)	0.05	10.52	0.35	3.51	-	-	14.43
Total emissions GWP-100 (kg CO_2e/kg H_2)	0.04	4.63	0.41	1.42	0.56	0.39	**7.4**
Total emissions GWP-20 (kg CO_2e/kg H_2)	0.07	11.54	0.64	3.72	0.56	0.39	**16.9**

Clean electricity scenario

To account for scope 2 emissions originating from the electric grid, the base case considers the 2021 annual average output emission rates by state from Environmental Protection Agency's eGRID [39], which is the most up-to-date version of emissions from the electric grid. For Texas and Ohio these emission rates are 0.39 and 0.55 kg CO_2e/kWh, respectively. However, this research also considers a scenario where electricity is obtained from low or zero-carbon energy sources, specifically wind power because this technology has the lowest life cycle emissions among other

renewable sources (0.011 kg CO_2e/kWh [40]). Figure 13 shows the life cycle GHG emissions for each case study based on a clean electricity scenario. The use of clean electricity decreases the life cycle GHG emissions of blue hydrogen by 22% for the Marcellus case and by 7% for the Permian case compared to the base cases, resulting in life cycle GHG emissions of 2.6 and 6.9 kg CO_2e/kg H_2, respectively. This difference in percentages of emissions reductions is due to the higher carbon intensity of the electric grid in Ohio compared to the electric grid in Texas, so the Permian case has a higher reduction in emissions.

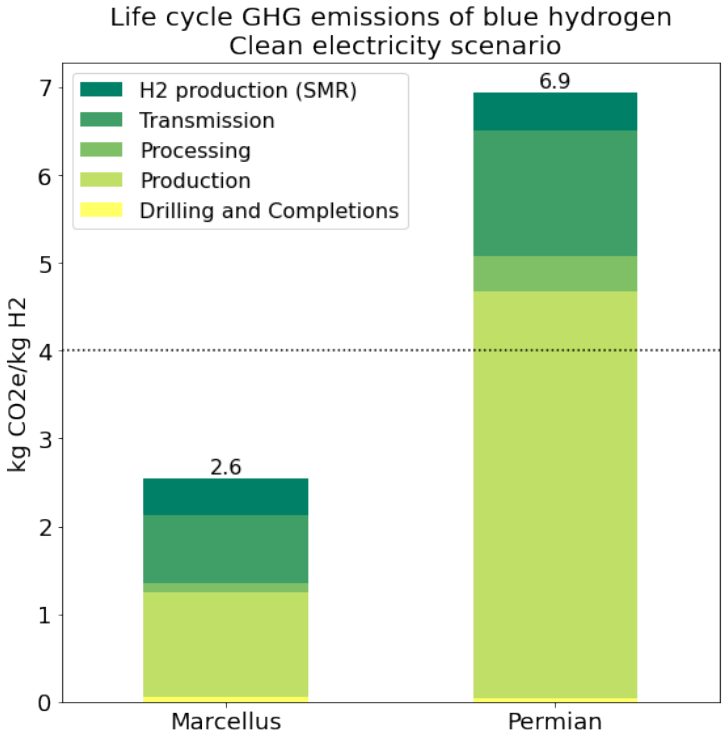

Figure S3: Clean electricity scenario - GHG emissions from blue hydrogen production using natural gas the Marcellus shale (left) and Permian basin (right), disaggregated across key life cycle stages (methane expressed in kg CO2e based on GWP of 100-year horizon from IPCC AR6). The dotted line represents the threshold to qualify for tax credits.

S10. Potential reduction in methane emissions

Due to the substantial contribution of methane emissions during upstream activities, a reduction in emissions could be achieved by decreasing the methane leakage from upstream activities. A total production-normalized methane emissions rate of 0.5%, would decrease life cycle GHG emissions to 2.5 kg CO_2e/kg H_2 for the Marcellus case, which is a 24% emissions reduction compared to the base-case scenario. For the Permian case, a reduction of production-normalized methane emissions rate to 0.5% reduces life cycle GHG emissions by 58% to 3.1 kg CO_2e/kg H_2 and this benchmark would qualify for the tax credits established by the IRA. The Permian case has a higher reduction in emissions because current measurement-based methane leakage estimates are substantially higher than in the Marcellus.

S11. Life Cycle Inventory (LCI) Parameters

Table S9. Emission factors.

Emission factors	Parameter	Units	Reference
CO_2 emission factor per scf of NG	5.49E-02	kg CO_2/scf NG	[42]
CO_2 emission factor per kg of NG	2.69E+00	kg CO_2/kg NG	[43]
Diesel emission factor	10.19	kg CO_2/gal diesel	[42]

Table S10. Global Warming Potential (GWP) for methane for 100 and 20 years.

Global Warming Potential	Parameter	Units	Reference
Methane (100-year)	27.9	kg CO_2e/kg CH_4	[44]
Methane (20-year)	81.2	kg CO_2e/kg CH_4	[44]

Marcellus shale

Table S11. Properties of wellhead and residue gas[45].

Parameter	Raw rich gas	Residue gas (pipeline quality)
Mol% C1	82.32	90.67
Mass fraction of methane	0.68	0.84
HHV (btu/scf)	1172.3	1077.9
LHV (btu/scf)	1082.2	975
Density (kg/m^3)	0.825	0.737
Density (kg/ft^3)	0.0234	0.0209

Table S12. Marcellus raw gas composition[45].

Component	Mol%	Mass fraction
N2	0.26	0.00
C1	82.32	0.68
C2	12.60	0.19
C3	3.18	0.07
NC4	0.68	0.02
IC4	0.38	0.01
NC5	0.15	0.01
IC5	0.27	0.01
C6	0.08	0.00
CO2	0.08	0.00
Total	100.00	1.00

Table S13. Marcellus residue gas composition[45].

Component	Mol%	Mass fraction
N2	0.29	0.00
C1	90.67	0.84
C2	8.77	0.15
C3	0.18	0.00
N-C4	0.00	0.00
I-C4	0.00	0.00
N-C5	0.00	0.00
I-C5	0.00	0.00
C6	0.00	0.00
CO2	0.09	0.00
Total	100.00	1.00

Table S14. Drilling and completions.

Parameter	Mean	Units	Reference
Methane volume emitted from well completion	251.85	Mscf/well/event	[46]
Flare destruction efficiency	98	%	[47]
Methane emissions from drilling	0.034	kg CH_4/s/well	[26]
Average drilling efficiency	22	days/well	[26]
Fuel used for drilling	16952	gal/well	[45]
Fuel used for fracturing	41235	gal/well	[45]

Table S15. Production-normalized methane emission rates from top-down studies in southwestern Marcellus.

Parameter	Low	Mean	High	Units	Reference
Methane emission rate per unconventional site	0.01	0.13	1.2	%	[28]
Natural gas flux/production rate	2.8	4.17	16.4	%	[26]
Methane emission rate (PA & WV)		1.1		%	[27]

Table S16. Inventory-derived emissions contribution from the natural gas supply chain[26].

Supply chain stage	Low (g CH_4/s/km^2)	Mean (g CH_4/s/km^2)	High (g CH_4/s/km^2)
Production	0.05	0.175	0.3
Processing	0.03	0.03	0.03
Local transmission	0.14	0.215	0.29
Local distribution	0.14	0.215	0.29
Interstate transmission	0.2	0.3025	0.405
Interstate distribution	0.2	0.3025	0.405
Total	0.76	1.24	1.72

Table S17. Emissions contribution per stage from top-down measurements estimated with data from Caulton et al.[26]

Supply chain stage	Mean emissions contribution (%)	Mean leakage rate	Mean leakage rate (with emissions below detection threshold)	Units
Production	14.11	0.59	0.63	%
Processing	2.42	0.10	0.10	%
Transmission	17.34	0.72	0.72	%
Total		1.41	1.46	%

Table S18. Emissions contribution per stage from top-down measurements estimated with data from Ren et al.[27]

Supply chain stage	Emissions contribution without distribution sector	Mean leakage rate (with emissions below detection threshold)	Units
Production	42	0.67	%
Processing	7	0.08	%
Transmission	51	0.56	%
Total	1.1	1.31	%

Table S19. Methane emissions from transmission and storage compressor stations estimated with data from Zimmerle et al[48]

Activity	% of total potential emissions	Units
Pipeline Leaks	0.13	%
Station	4.51	%
Reciprocating Compressor	31.42	%
Dehydrator vents	0.08	%
Exhaust from engines	9.56	%
Generators (engines)	0.47	%
Pneumatic Devices	8.99	%
Pipeline venting (routine maintenance)	7.51	%
Station venting	6.14	%
Mean total transmission and storage emission rate	0.35	%
Emissions contribution for transmission compressor stations (no storage)	61.17	%
Emissions contribution for transmission pipelines (no storage)	7.64	%
Mean total emission rate from transmission compressor stations	0.2141	%
Mean total emission rate from transmission pipelines	0.0267	%

Table S20. Production – Upstream activities

Parameter	Mean	Units	Reference
Estimated Ultimate Recovery (EUR)	5.12	Bcf/well	[45]
Methane leakage rate from production (upstream)	0.64	NG loss/production rate (%)	[26]
Methane leakage rate from production (upstream)	0.70	NG loss/production rate (%)	[27]
Liquids Unloading (throughput normalized methane emissions)	0.059	kg CH_4/kg CH_4 produced (%)	[49]
Fuel use for compression	2.2	scf fuel gas/scf throughput (%)	[45]
Fuel for dehydration, other operations	0.12	scf fuel gas/scf throughput (%)	[45]

Table S21. Natural gas processing.

Parameter	Mean	Units	Reference
Raw Marcellus gas feed to facility	131.52	MMscf/day	[45]
Gross flow of pipeline quality gas leaving facility	119.03	MMscf/day	[45]
Natural gas plant liquids yield	72	b/MMcf	[37]
Energy density of natural gas liquids (NGL)	3.82	MMBTU/bbl	[50]
Methane leakage rate from processing	0.10	Fugitive NG loss/production rate (%)	[26]
Methane leakage rate from processing	0.08	Fugitive NG loss/production rate (%)	[27]
Facility fuel gas consumption	0.25	MMscf/day	[45]

Table S22. Estimated methane leakage rates from transmission facilities.

Parameter	Mean	Units	Reference
Methane leakage rate (compressor stations)	0.72	NG loss/production rate (%)	[26]
Methane leakage rate (compressor stations)	0.56	NG loss/production rate (%)	[27]
Methane leakage rate from (compressor stations and pipelines)	0.24	NG loss/production rate (%)	[48]

Table S23. Operational parameters for CO_2 injection.

Parameter	Mean	Units	Reference
Pressure drop along CO_2 transportation pipeline	0.1276	MPa/mile	[51]
Normal pressure gradient	0.433	psi/ft	[52]
Average depth for injection in Maryville formation (Ohio)	7000	ft	[53]
Average injection pressure	20.9	MPa	
Power requirement for CO_2 injection	667.18	kW	
Normalized power requirement for CO_2 injection	0.03	kWh/kg H_2	

Permian basin

Table S24. Properties of wellhead and residue gas[54].

Parameter	Raw gas	Residue gas (pipeline quality)
Mol% C1	72.07	97.10
Mass fraction of methane	0.50	0.95
HHV (btu/scf)	1235	981
LHV (btu/scf)		884
Molecular weight (g/mol)		16.39
Density (kg/m3)	0.774	0.695
Density (kg/ft3)	0.0219	0.0197

Table S25. Permian raw gas composition.

Component	Mol%	Mass fraction
N2	2.09	0.03
C1	72.07	0.50
C2	12.12	0.16
C3	6.15	0.12
NC4	1.86	0.05
IC4	0.73	0.02
NC5	0.50	0.02
IC5	0.46	0.01
C6	1.27	0.05
CO2	2.75	0.05
Total	100.00	1.00

Table S26. Permian residue gas composition (ethane recovery).

Component	Mol%	Mass fraction
N2	2.80	0.05
C1	97.10	0.95
C2	0.10	0.00
C3	0.00	0.00
N-C4	0.00	0.00
I-C4	0.00	0.00
N-C5	0.00	0.00
I-C5	0.00	0.00
C6	0.00	0.00
CO2	0.00	0.00
Total	100.00	1.00

Table S27. Drilling and completions.

Parameter	Mean	Units	Reference
Methane volume emitted from well completion	130.46	Mscf/well/event	[47]
Flare destruction efficiency	98	%	[26]
Methane emissions from drilling	0.034	kg CH_4/s/well	[26]
Average drilling efficiency	22	days/well	[26]
Fuel used for drilling	53730	gal/well	[55]
Fuel used for fracturing	23402	gal/well	[55]

Table S28. Production-normalized methane emission rates from top-down studies in the Permian basin.

Parameter	Mean	Units	Reference
Methane emission rate New Mexico Permian basin	9.4	%	[20]
Methane emission rate derived via TROPOMI observations	3.7	%	[18]

Table S29. Emissions contribution per stage from top-down measurements estimated with data from Chen et al. [20]

Supply chain stage	Emissions contribution	Mean emission rate	Units
Production	52	4.89	%
Processing	2	0.19	%
Transmission	17	1.60	%

Table S30. Emissions contribution per stage from top-down measurements estimated with data from Zhang et al.[18]

Supply chain stage	Site-level emissions (Tg/yr)	Emissions contribution (%)	Mean leakage rate (%)
Production	2.30	86	3.20
Processing	0.14	5	0.19
Transmission	0.22	8	0.31
Total	2.66		

Table S31. Production – Upstream activities

Parameter	Mean	Units	Reference
Methane leakage rate from production	4.89	NG loss/production rate (%)	[20]
Methane leakage rate from production	3.2	NG loss/production rate (%)	[18]
Liquids Unloading (throughput normalized methane emissions)	0.0093	kg CH4/kg CH4 produced (%)	[49]
Fuel consumption in the production facility	475	Mscf NG/facility-yr	[56]
Fuel consumption for compression (G&B)	1.16E+11	scf NG/facility-yr	[56]
Production rate per production facility	4.47E+11	scf/facility-yr	[56]
Natural gas throughput in the gathering and boosting facility	2.31E+12	scf/yr	[56]

Table S32. Permian basin yearly production and energy density of fluids for energy-based allocation.

Parameter	Mean	Units	Reference
Oil Production Volume	1,079,185,794	bbl/year	[36]
Casinghead Production Volume	3.13396E+12	scf/year	[36]
Gas Production Volume	1.85865E+12	scf/year	[36]
Condensate Production Volume	187,444,378	bbl/year	[36]
Energy density of oil	5.8	MMBTU/bbl	[50]
Energy density of gas	1,235	BTU/scf	[50]
Gas Oil Ratio	8,000	scf/bbl	[13]

Table S33. Natural gas processing.

Parameter	Mean	Units	Reference
Flowrate of gas feed to CDP	200	MMscf/day	[54]
Flowrate of residue gas recycled to cryo inlet in ethane recovery mode	19.5	MMscf/day	[54]
Methane leakage rate from processing	0.19	NG loss/Mcg NG (%)	[20]
Methane leakage rate from processing	0.2	NG loss/Mcg NG (%)	[18]
Natural gas throughput	3.36E+10	scf NG/facility-yr	[56]
Fuel Consumption	7.72E+08	scf NG/facility-yr	[56]
Natural Gas Plant Liquids Production	95	b/MMcf	[37]
Energy density of natural gas liquids (NGL)	3.82	MMBTU/bbl	[50]

Table S34. Natural gas transmission.

Parameter	Mean	Units	Reference
Flowrate of residue gas	1.81E+08	scf/day	[56]
Methane leakage rate (compressor stations)	1.60	NG loss/production rate (%)	[20]
Methane leakage rate (compressor stations)	0.31	NG loss/production rate (%)	[18]
Methane leakage rate (compressor stations and pipelines)	0.24	NG loss/production rate (%)	[48]

Table S35. Operational parameters of transmission compressor stations in the U.S.

Parameter	Mean	Units	Reference
Share of reciprocating engines (gas-powered)	78	%	[57]
Share of centrifugal engines (gas-powered)	19	%	[57]
Share of centrifugal engines (electrical)	3	%	[57]
Average horsepower capacity of reciprocating compressors	2335.00	hp	[58]
Thermal efficiency of reciprocating compressors	37.50	%	[48]
Average number of centrifugal compressor units per station	5.00	compressor units	[58]
Average operating hours per compressor unit	2914.00	hours/year	[48]
Average distance between transmission compressor stations	75.00	mi	[57]

Table S36. Parameters to calculate power requirement for CO_2 compression and pumping[59].

Parameter	Value	Units
Number of compression stages	5.00	
Gas constant (R)	8.31	kJ/kmol-K
Molecular weight CO_2 (M)	44.01	kg/kmol
CO_2 temperature at compressor inlet (T)	313.15	K
Isentropic efficiency of compressor (n)	0.75	
CO_2 mass flow rate to be transported (m)	4618.00	tonnes/day
Initial pressure	0.10	MPa
Critical pressure	7.38	MPa
Final pressure	15.00	MPa
Optimal compression ratio	0.49	
Density of liquid CO_2	630.00	kg/m^3

Table S37. Average CO_2 compressibility and ratio of specific heats per stage[59].

Stage	CO_2 compressibility	Ratio of specific heats of CO_2 (Cp/Cv)
1	0.995	1.277
2	0.985	1.286
3	0.97	1.309
4	0.935	1.379
5	0.845	1.704

Table S38. Power requirement for CO_2 compression per stage and pumping[59].

Compression stage	Compression power requirement (kW)
1	2757.71
2	2724.83
3	2670.71
4	2540.24
5	2190.20
Total compression power requirement	12883.69
Pumping power requirement	229.92
Total compression and pumping power	13113.61

Table S39. Operational parameters of SMR plant with CO_2 capture and compression.

Parameter	Amount	Units	Reference
Molar mass CH_4	16.04	g/mol	
Molar mass H_2	2.02	g/mol	
Molar mass CO_2	44.01	g/mol	
Molar mass CO	28.01	g/mol	
Molar mass H_2O	18.01	g/mol	
Methane density at standard conditions	0.019	kg/ft^3	[60]
Heating value of methane	1010	BTU/scf	[61]
Moles H_2/mole CH_4	4	mol H_2/mol CH_4	
Moles CO_2/mole CH_4	1	mol CO_2/mol CH_4	
HHV hydrogen	134476.3	BTU/kg H_2	[62]
Power for SMR	7070	kW	
Power for CO_2 capture/Removal Auxiliaries	6710	kW	
Power for CO_2 compression	13113.61	kW	
Total power	26893.61	kW	
V-L flowrate H_2 product	20,125	kg/h	[38]
Cold gas efficiency for SMR with CO_2 capture	72.1	%	[38]
Natural gas feed flowrate to SMR plant	75,472	kg/hr	[38]
Fuel flowrate to SMR plant	11,588	kg/hr	[38]
Carbon capture rate (base case)	96.2	%	[38]

Table S40. Average GHG emission rates from electricity grid and wind power.

Source	GHG emission rate	Units	Reference
Ohio	0.551	kg CO_2e/kWh	[39]
Texas	0.390	kg CO_2e/kWh	[39]
Wind power	0.011	kg CO_2e/kWh	[40]

Table S41. Operational parameters for CO_2 injection.

Parameter	Mean	Units	Reference
Pressure drop along CO_2 transportation pipeline	0.1276	MPa/mile	[51]
Normal pressure gradient	0.433	psi/ft	[52]
Average formation depth for CO_2 injection in Texas	6500	ft	[63]
Average injection pressure	20.9	MPa	
Power requirement for CO_2 injection	667.18	kW	
Normalized power requirement for CO_2 injection	0.03	kWh/kg H_2	

References

1. Rep. Yarmuth, J. A. [D-K.-3. Text - H.R.5376 - 117th Congress (2021-2022): Inflation Reduction Act of 2022. http://www.congress.gov/ (2022).

2. ISO 14040:2006(en), Environmental management — Life cycle assessment — Principles and framework. https://www.iso.org/obp/ui/#iso:std:iso:14040:ed-2:v1:en.

3. Where our natural gas comes from - U.S. Energy Information Administration (EIA). https://www.eia.gov/energyexplained/natural-gas/where-our-natural-gas-comes-from.php.

4. Frequently Asked Questions (FAQs) - U.S. Energy Information Administration (EIA). https://www.eia.gov/tools/faqs/faq.php.

5. Popova, O. Marcellus Shale Play. (2017).

6. Natural Gas Processing Plants. https://hifld-geoplatform.opendata.arcgis.com/datasets/ca984888f8154c63bf3a023f0a1f9ac2_0/explore.

7. Natural Gas Compressor Stations. https://hifld-geoplatform.opendata.arcgis.com/datasets/cb4ea4a90a5e4849860d0d56058c2f75_0/explore?location=36.933237,-96.043033,5.38.

8. Geospatial Data Science Applications and Visualizations. https://maps.nrel.gov/?da=hydra.

9. Ohio Enhanced Oil Recovery Class II Injection Wells - Overview. https://ut-austin.maps.arcgis.com/home/item.html?id=e58ad80a9dc04bc3801c66a94676ce77.

10. Natural Gas Interstate and Intrastate Pipelines - Overview. https://ut-austin.maps.arcgis.com/home/item.html?id=4a158d2113f145039f71b80d07e2c19c.

11. permian.pdf. https://www.eia.gov/petroleum/drilling/pdf/permian.pdf.

12. Permian Basin Oil and Gas Overview | Enverus. https://www.enverus.com/permian-basin/.

13. Advances in technology led to record new well productivity in the Permian Basin in 2021. https://www.eia.gov/todayinenergy/detail.php?id=54079.

14. CO2_wells_TX - Overview. https://ut-austin.maps.arcgis.com/home/item.html?id=3c39e8d5be3047bdae94206a0c829635.

15. Shaw, J. T., Shah, A., Yong, H. & Allen, G. Methods for quantifying methane emissions using unmanned aerial vehicles: a review. *Philos. Transact. A Math. Phys. Eng. Sci.* **379**, 20200450.

16. Vaughn, T. L. *et al.* Temporal variability largely explains top-down/bottom-up difference in methane emission estimates from a natural gas production region. *Proc. Natl. Acad. Sci.* **115**, 11712–11717 (2018).

17. Rutherford, J. S. *et al.* Closing the methane gap in US oil and natural gas production emissions inventories. *Nat. Commun.* **12**, 4715 (2021).

18. Zhang, Y. *et al.* Quantifying methane emissions from the largest oil-producing basin in the United States from space. *Sci. Adv.* **6**, eaaz5120 (2020).

19. Leyden, C. New report: Routine flaring in Texas' Permian can be eliminated at little to no cost. *Energy Exchange* https://blogs.edf.org/energyexchange/2021/01/26/new-report-routine-flaring-in-texas-permian-can-be-eliminated-at-little-to-no-cost/ (2021).

20. Chen, Y. *et al.* Quantifying Regional Methane Emissions in the New Mexico Permian Basin with a Comprehensive Aerial Survey. *Environ. Sci. Technol.* **56**, 4317–4323 (2022).

21. Schneising, O. *et al.* Remote sensing of methane leakage from natural gas and petroleum systems revisited. *Atmospheric Chem. Phys.* **20**, 9169–9182 (2020).

22. Lyon, D. R. *et al.* Concurrent variation in oil and gas methane emissions and oil price during the COVID-19 pandemic. *Atmospheric Chem. Phys.* **21**, 6605–6626 (2021).

23. Dubey, L., Cooper, J. & Hawkes, A. Minimum detection limits of the TROPOMI satellite sensor across North America and their implications for measuring oil and gas methane emissions. *Sci. Total Environ.* **872**, 162222 (2023).

24. Brandt, A. R., Heath, G. A. & Cooley, D. Methane Leaks from Natural Gas Systems Follow Extreme Distributions. *Environ. Sci. Technol.* **50**, 12512–12520 (2016).

25. Frankenberg, C. *et al.* Airborne methane remote measurements reveal heavy-tail flux distribution in Four Corners region. *Proc. Natl. Acad. Sci.* **113**, 9734–9739 (2016).

26. Caulton, D. R. *et al.* Toward a better understanding and quantification of methane emissions from shale gas development. *Proc. Natl. Acad. Sci.* **111**, 6237–6242 (2014).

27. Ren, X. *et al.* Methane Emissions from the Marcellus Shale in Southwestern Pennsylvania and Northern West Virginia Based on Airborne Measurements. *J. Geophys. Res. Atmospheres* **124**, 1862–1878 (2019).

28. Omara, M. *et al.* Methane Emissions from Conventional and Unconventional Natural Gas Production Sites in the Marcellus Shale Basin. *Environ. Sci. Technol.* **50**, 2099–2107 (2016).

29. Omara, M. *et al.* Methane Emissions from Natural Gas Production Sites in the United States: Data Synthesis and National Estimate. *Environ. Sci. Technol.* **52**, 12915–12925 (2018).

30. Barkley, Z. *et al. Quantification of Oil and Gas Methane Emissions in the Delaware and Marcellus Basins Using a Network of Continuous Tower-Based Measurements*. https://acp.copernicus.org/preprints/acp-2022-709/ (2022) doi:10.5194/acp-2022-709.

31. Wang, J. L. *et al.* Multiscale Methane Measurements at Oil and Gas Facilities Reveal Necessary Frameworks for Improved Emissions Accounting. *Environ. Sci. Technol.* **56**, 14743–14752 (2022).

32. Esparza, Á. E. *et al.* Analysis of a tiered top-down approach using satellite and aircraft platforms to monitor oil and gas facilities in the Permian basin. *Renew. Sustain. Energy Rev.* **178**, 113265 (2023).

33. Zavala-Araiza, D., Allen, D. T., Harrison, M., George, F. C. & Jersey, G. R. Allocating Methane Emissions to Natural Gas and Oil Production from Shale Formations. *ACS Sustain. Chem. Eng.* **3**, 492–498 (2015).

34. Aldrich, R., Llauró, F. X., Puig, J., Mutjé, P. & Pèlach, M. À. Allocation of GHG emissions in combined heat and power systems: a new proposal for considering inefficiencies of the system. *J. Clean. Prod.* **19**, 1072–1079 (2011).

35. CHP_guidance_v1.0.pdf. https://ghgprotocol.org/sites/default/files/CHP_guidance_v1.0.pdf.

36. General Production Query Criteria. https://webapps2.rrc.texas.gov/EWA/productionQueryAction.do;jsessionid=u8qajKF0X9fcwswJ94iK8uCB-VBx1fsPQlPb7p-Jb9vIeWS2JOEK!778911444.

37. U.S. natural gas plant liquid production continues to hit record highs. https://www.eia.gov/todayinenergy/detail.php?id=38772.

38. Lewis, E. *et al. Comparison of Commercial, State-of-the-Art, Fossil-Based Hydrogen Production Technologies*. DOE/NETL-2022/3241, 1862910 https://www.osti.gov/servlets/purl/1862910/ (2022) doi:10.2172/1862910.

39. eGRID2021_summary_tables.pdf. https://www.epa.gov/system/files/documents/2023-01/eGRID2021_summary_tables.pdf.

40. Dolan, S. L. & Heath, G. A. Life Cycle Greenhouse Gas Emissions of Utility-Scale Wind Power. *J. Ind. Ecol.* **16**, S136–S154 (2012).

41. van Renssen, S. The hydrogen solution? *Nat. Clim. Change* **10**, 799–801 (2020).

42. U.S. Energy Information Administration - EIA - Independent Statistics and Analysis. https://www.eia.gov/environment/emissions/co2_vol_mass.php.

43. Calculation Tools | GHG Protocol. https://ghgprotocol.org/calculation-tools#cross_sector_tools_id.

44. IPCC_AR6_WGI_Chapter_07_Supplementary_Material.pdf. https://www.ipcc.ch/report/ar6/wg1/downloads/report/IPCC_AR6_WGI_Chapter_07_Supplementary_Material.pdf.

45. Mallapragada, D. S. *et al.* Life cycle greenhouse gas emissions and freshwater consumption of liquefied Marcellus shale gas used for international power generation. *J. Clean. Prod.* **205**, 672–680 (2018).

46. Allen, D. T. *et al.* Measurements of methane emissions at natural gas production sites in the United States. *Proc. Natl. Acad. Sci.* **110**, 17768–17773 (2013).

47. 13.5_industrial_flares.pdf. https://www.epa.gov/sites/default/files/2020-10/documents/13.5_industrial_flares.pdf.

48. Zimmerle, D. J. *et al.* Methane Emissions from the Natural Gas Transmission and Storage System in the United States. *Environ. Sci. Technol.* **49**, 9374–9383 (2015).

49. Zaimes, G. G. *et al.* Characterizing Regional Methane Emissions from Natural Gas Liquid Unloading. *Environ. Sci. Technol.* **53**, 4619–4629 (2019).

50. Roman-White, S. A. *et al.* LNG Supply Chains: A Supplier-Specific Life-Cycle Assessment for Improved Emission Accounting. *ACS Sustain. Chem. Eng.* **9**, 10857–10867 (2021).

51. Energy Analysis. *netl.doe.gov* https://netl.doe.gov/energy-analysis/details.

52. pressure_gradient. https://glossary.slb.com/en/terms/p/pressure_gradient.

53. Cumming, L., Hawkins, J., Sminchak, J., Valluri, M. & Gupta, N. Researching candidate sites for a carbon storage complex in the Central Appalachian Basin, USA. *Int. J. Greenh. Gas Control* **88**, 168–181 (2019).

54. Contreras, W. *et al.* Life cycle greenhouse gas emissions of crude oil and natural gas from the Delaware Basin. *J. Clean. Prod.* **328**, 129530 (2021).

55. Laurenzi, I. J., Bergerson, J. A. & Motazedi, K. Life cycle greenhouse gas emissions and freshwater consumption associated with Bakken tight oil. *Proc. Natl. Acad. Sci.* **113**, E7672–E7680 (2016).

56. Roman-White, S., Rai, S., Littlefield, J., Cooney, G. & Skone, T. J. LIFE CYCLE GREENHOUSE GAS PERSPECTIVE ON EXPORTING LIQUEFIED NATURAL GAS FROM THE UNITED STATES: 2019 UPDATE.

57. Skone, T. J., Littlefield, J. & Marriott, J. *Life Cycle Greenhouse Gas Inventory of Natural Gas Extraction, Delivery and Electricity Production*. NETL/DOE--2011/1522, 1515238 http://www.osti.gov/servlets/purl/1515238/ (2011) doi:10.2172/1515238.

58. Subramanian, R. *et al.* Methane Emissions from Natural Gas Compressor Stations in the Transmission and Storage Sector: Measurements and Comparisons with the EPA Greenhouse Gas Reporting Program Protocol. *Environ. Sci. Technol.* **49**, 3252–3261 (2015).

59. McCollum, D. L. & Ogden, J. M. Techno-Economic Models for Carbon Dioxide Compression, Transport, and Storage & Correlations for Estimating Carbon Dioxide Density and Viscosity.

60. Thermophysical Properties of Fluid Systems. https://webbook.nist.gov/chemistry/fluid/.

61. U.S. Energy Information Administration - EIA - Independent Statistics and Analysis. https://www.eia.gov/todayinenergy/detail.php?id=18371.

62. *Read 'The Hydrogen Economy: Opportunities, Costs, Barriers, and R&D Needs' at NAP.edu*. doi:10.17226/10922.

63. SACROC Research Project | Bureau of Economic Geology. https://www.beg.utexas.edu/gccc/research/sacroc.